water

MDPI

Article

Mesoscale Rhythmicity of Zooplankton Concentration in Various Aquatic Environments Based on Data from a Submersible Digital Holographic Camera

Victor Dyomin, Alexandra Davydova *, Nikolay Kirillov and Igor Polovtsev

Laboratory of Radiophysical and Optical Methods for Environmental Research, National Research Tomsk State University, Tomsk 634050, Russia; dyomin@mail.tsu.ru (V.D.); knsnik@gmail.com (N.K.); polovcev_i@mail.ru (I.P.)

* Correspondence: starinshikova@mail.ru

Abstract

The paper explores the application of a submersible digital holographic camera for studying the mesoscale dynamics of zooplankton concentrations across various aquatic ecosystems. The spectral analysis of the time series of zooplankton concentrations measured by the developed submersible digital holographic camera showed that zooplankton communities in all studied water areas are characterized by a discrete linear Fourier spectrum with corresponding c-circadian (24 h), dv-semidiurnal (12 h) and lf-low frequency components of variability. These rhythmic patterns are observed or present across aquatic environments that substantially differ in taxonomic composition and habitat conditions, including Lake Bolshoye Yarovoe (Altai), Lake Baikal, the Barents Sea, and the Central Arctic Basin. In all these waters, monitoring measurements of zooplankton concentrations were performed using underwater holography. It was shown that regional lf-rhythms reflecting a low-frequency component may disable diagnostic c- and dv-rhythms, but could be effectively separated through segmentation and trend correction. The paper suggests a three-component harmonic model based on lf-, c- and dv-rhythms. Stress tests (simulation of pollution and organic waste discharge) showed that the environmental imbalance shifts the spectral lines, increases the high-frequency components and the model error. The high sensitivity of diagnostic biorhythms to external influences makes it possible to use the discrepancy of the model with plankton concentrations measured using a submersible digital holographic camera as early indicators of environmental distress for non-invasive real-time monitoring of aquatic ecosystems.

Keywords: digital holographic camera; zooplankton; bioindication; biorhythms; time series analysis; Fourier spectrum; environmental monitoring; Lake Baikal; Barents Sea

Academic Editor: Genuario Belmonte

Received: 15 October 2026
Revised: 13 November 2026
Accepted: 25 November 2026
Published: 27 November 2026

Copyright: © 2026 by the author. Licensee MDPI, Basel, Switzerland. This article is an open access article distributed under the terms and conditions of the Creative Commons Attribution (CC BY) license.

1. Introduction

Plankton in general and zooplankton in particular play a critical role in the following processes:

- carbon cycle and circulation of substances in the ocean [1–3];
- ecosystem food chain being almost at its base [4,5];
- natural self-purification of water bodies due to filtration feeding [6–10];

- illustration of self-organization and the evolutionary capacity of biocenoses [11–14];
- assessment of the water quality index, reflecting the anthropogenic impact in the ocean [15–23].

Zooplankton is present in any water body and water area and is in a state of ecological equilibrium with the living conditions, which allows it to be used for bioindication of the ecosystem [22,24,25]. This is expressed in characteristic zooplankton biorhythms [26–34], the failure of which can be an indicator of environmental disturbance.

Here the rhythmics of zooplankton concentrations (or systematic component of variability) in a particular place and at a certain period of time is the result of the interaction of natural fluctuations in the number of zooplankton biocenosis and the impact of environmental factors. Intrinsic (internal) fluctuations are caused by biological factors: sleep–wake cycles, feeding cycles, reproductive cycles, predator-prey interactions [35–37], and occur, as in physics, due to the internal energy of the population having a biological nature [38]. They are fed from external abiotic factors characterized by an impact force, such as sunlight, gravitational, hydrochemical and hydrophysical phenomena, wind load [27,39,40].

The interaction of intrinsic fluctuations with impact forces is quite resonant, which is confirmed by the fact that, when viewed spectrally, the rhythms of zooplankton concentrations are shown as spectral lines having a scale corresponding to the process period, and therefore we are talking about modalities, i.e., about different types and scales (modes) of the corresponding rhythm. Thus, for instance, the circadian rhythm line is observed in mesoscale modality. Inhomogeneities of this type are generated by biotic interactions of daily duration initiated by the illumination factor, which are corrected by inertial and tidal movements in the ocean, daily fluctuations in the intensity of the thermodynamic interaction of the ocean and atmosphere.

The time series of measurements of zooplankton concentrations is formed and segmented accordingly, while establishing the duration of measurements and the studied volume of the zooplankton group. In the process of long-term monitoring, when the most representative series of zooplankton concentrations is formed for the rhythm analysis, it becomes necessary to divide this series into shorter intervals (here referred to as segments) for the purpose of operational and therefore timely analysis. The segmentation of time series is a tool for the selection of spatial and temporal scales to describe interactions and choose the spectral band (modality) of the studied biorhythms [41].

To detect rhythms in the mesoscale modality, the segment duration $2T$ may be $72\ \text{h} < 2T < 240\ \text{h}$. When this duration is chosen, the reliability of the results should be used to identify the systematic component of variability.

Since the above external factors are planetary phenomena, the observed resonant phenomena caused by the interaction of natural vibrations and external factors should appear everywhere, in any water area. Therefore, the circadian rhythm, or c-rhythm (associated with sunrise and sunset) and the semidiurnal variability rhythm, or dv-rhythm (associated with the nutrition cycle), allow ecological interpretation as a systematic component of variability, and are considered diagnostic here, since they are realized by zooplankton independently and on the scale of the entire water area, due to the planetary scale of the coercive force.

The regional specific nature of the structuring rhythms (s-rhythms) is determined in the area of intrinsic fluctuations of water bodies associated with a change in wind directions and currents in dynamic models of water bodies [42–45]. It is logical to seek for the cause of s-rhythm in non-stationary parts of models, such as surface and internal waves created by air and water movements [46].

If we consider the synoptic modality, s-rhythms are easily eliminated from monitoring results [41]. This is explained by the fact that the modalities caused by synoptic

phenomena are characterized by larger time scales compared with the period of s-rhythms—decades, months, seasons. If the regional s-rhythm is observed in the mesoscale region (with time scales corresponding to hours and days), then it may affect the diagnostic intrinsic rhythms (spectral lines). Such regional rhythms, penetrating the mesoscale band and affecting the diagnostic rhythms, are called here the lf-rhythms. Being a kind of structuring rhythms, lf-rhythms affect the concentrations of plankton through diffusion caused by turbulent energy-bearing Kolmogorov vortices [41], therefore they have no ecological interpretation as a random component of variability. As a consequence, the influencing properties of such rhythms on the diagnostic rhythms should be minimized.

Let us formulate the main hypotheses supported in this work based on several examples.

1. The results of Fourier spectral processing of the time series of concentrations of free-living plankton demonstrate the presence of a systematic component in the behavior of the autochthonous plankton community. This constituent is identified as diagnostic biorhythms of semidiurnal variability in the zooplankton community associated with sleep–wake processes and daily nutrition. These processes are vital, so appropriate rhythms are considered fundamental and are present in any water body.
2. Several days of measurements are sufficient to determine the parameters of vital rhythms of semidiurnal variability and check their stability, which confirms the transition from a continuous series of monitoring measurements to time segments. Moreover, it is enough to monitor a small number (usually two diagnostic rhythms) of biorhythms to assess the state of the ecosystem.
3. Disruption of the structure of vital rhythms indicates the environmental degradation of biocenosis. For example, significant changes in the parameters of diagnostic biorhythms indicate habitat discomfort associated with pollution. This is illustrated in the paper through a stress test based on a substantial change in water quality simulating anthropogenic impact. In addition, there is a need for mathematical methods to separate the influence of lf-rhythms on the structure of diagnostic rhythms.

The recorded change in the rhythmic parameters of semidiurnal variability of zooplankton biocenosis under the influence of this stressor makes it possible to use the behavior of autochthonous zooplankton as a bioindicator of pollution. Furthermore, the generality of diagnostic rhythms and specific anomalies of the spectra of zooplankton concentration variability is shown on the example of several water areas, even in water areas that are widely different in zooplankton taxonomy and its existence conditions.

This study suggests the possibility of using in situ hardware imaging system operating for a long time in a submersible state. Such systems [47–49] are currently quite popular due to the efficiency of data acquisition and the possibility of differential measurements without interfering with biocenosis. These capabilities allow visualization systems to have significant advantages over traditional integrated catching methods [50,51]. DHC technologies hold a special place among in situ imaging systems due to the simplicity of the optical scheme, weight and size ratios and the ability to register a 'portrait' of all particles in the working volume [52,53]. Such submersible digital holographic cameras as a non-disturbing method for direct measurement of plankton in the habitat are used to study the rhythmic processes and methods of processing holographic data due to bioindication of pollution.

The principal contribution of this work is a comparative generalization of experimental data in the context of the above theses. This required the additional analysis of earlier obtained data. At the same time, the following information was previously published [41,54–57]:

- DHC design and holographic recording technique;

- fundamental concept of the Fourier representation of the systematic component of plankton concentration variability;
- deployment systems and separate data sets for Bolshoye Yarovoye Lake, summer moorage on Lake Baikal and the Barents Sea.

These papers also present preliminary observations of spectral components and shift of spectral lines under disturbance.

The following novel data are presented in this manuscript:

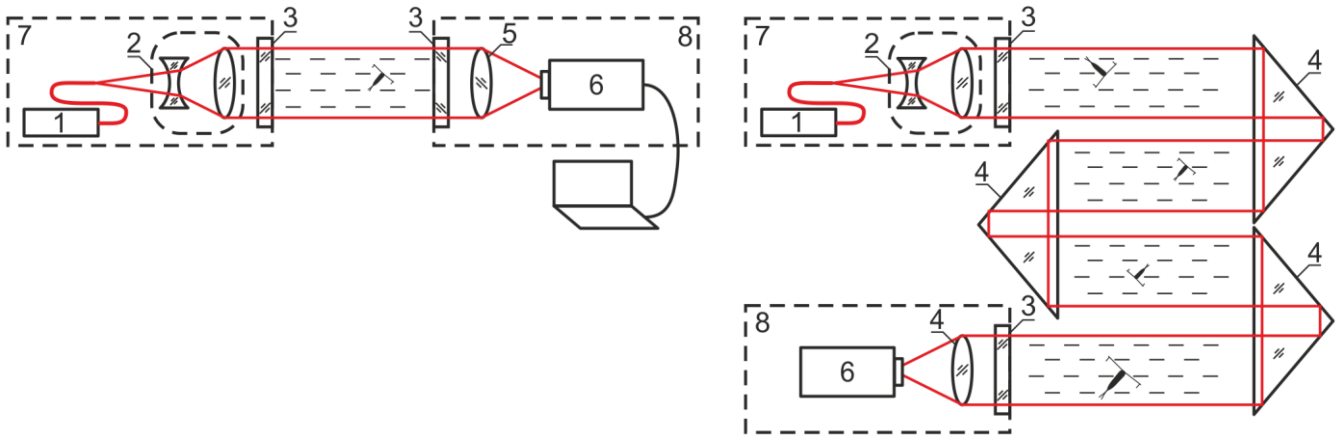
- single three-component harmonic model (lf + c + dv), applied and combined for plankton measurements in five water areas, including the first published data obtained in winter 2022 in Lake Baikal and data obtained during the arctic drift of the ice-resistant platform SP-42 (2024–2025);
- quantitative segmentation and local correction of plankton concentration trend, which allows separating lf-rhythm from diagnostic lines;
- two stress tests and a model mismatch metric as an indicator of rhythm disturbance;
- generalization regarding the interaction of c- and dv-rhythms during the following transition: polar day → polar night and vice versa.

2. Materials and Methods

2.1. DHC-Based Equipment of Bioindication Station

A digital holographic camera (DHC, manufactured by TSU, Tomsk, Russia) was used in this study to monitor plankton concentrations. Its design and data processing methods are described in the works [41,54–57].

The registration scheme using the Gabor in-line holography within the DHC is shown in Figure 1 [57]. Collimated beam of coherent light from laser diode (1) illuminates the volume of water medium with particles of different nature (plankton, settling particles, bubbles, drops, etc.). An object wave field is formed as a result of the light scattering on the particles. It interacts with the illuminating field, forming an interference pattern. This interference pattern is recorded by the matrix of the CMOS camera (6) as a two-dimensional array of intensity values, which is a digital hologram of the working volume. To reduce the size of the device, prisms (4) are placed into the optical scheme ensuring the "folded" configuration of the Gabor in-line scheme and forming a measuring (working) volume. The laser, optical and electronic components forming the illuminating beam and located in the sealed case constitute the illuminating unit (7). Camera, optical and electronic components ensuring hologram recording are part of the recording unit (8).



(**a**) (**b**)

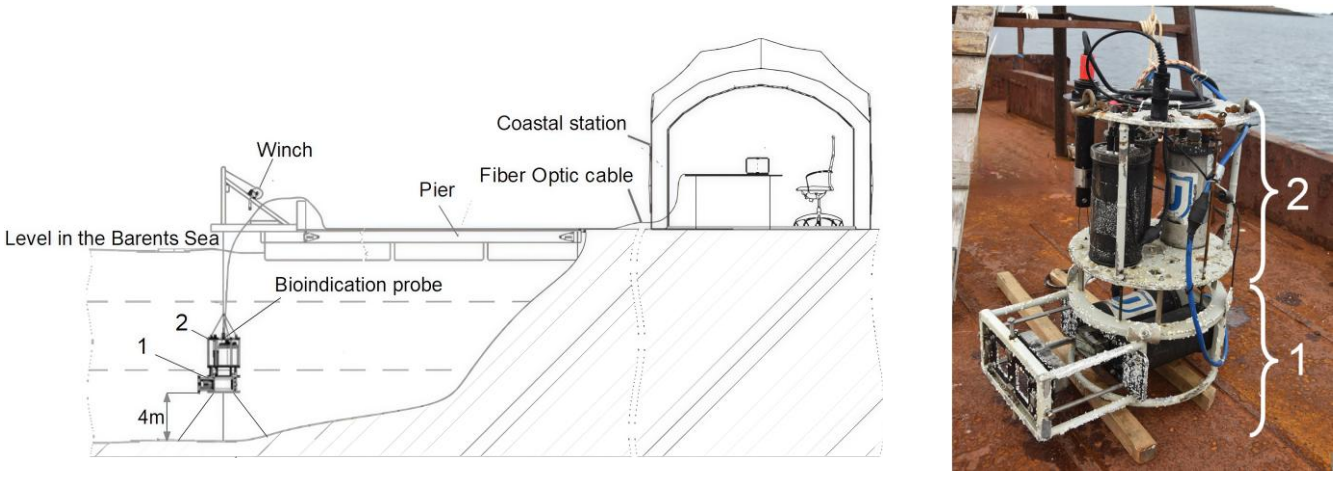
Figure 1. DHC operating principle (adapted from [57]): (**a**) Gabor scheme for suspended particle recording, (**b**) submersible DHC layout. 1—laser diode with fiber-coupled output, 2—beam

expander (Galileo scheme), 3—portholes, 4—mirror-prism system that forms the measuring (working) volume, 5—lens, 6—CMOS camera, 7—illuminating unit, 8—recording unit. Red lines point the direction of laser light propagation.

For field studies, the DHC is assembled together with medium sensors (pressure, temperature, electrical conductivity, illumination) and an information unit into a hydrobiological DHC-FOCL probe (FOCL—Fiber Optical Communication Line) operating according to a network principle. The on-board computer of the information unit enables real-time, in situ recording of data on the disk with further transmission via a FOCL communication channel to an onshore or ship computer station, where the hologram stream is processed and the measurement series are formed.

2.2. Deployment and Sampling System

This study uses the monitoring data obtained at fixed bioindication stations placed at a fixed height from the bottom in various water areas. Figure 2 shows an example of such arrangement on a pontoon pier [57].



(**a**) (**b**)

Figure 2. Moorage of the DHC-FOCL probe in Dalnye Zelentsy settlement. N 69°7′7.9″ E 36°4′10″, (**a**) general location plan and device layout (adapted from [57]). (**b**) general view of the DHC-FOCL probe for plankton monitoring. 1—DHC, 2—information unit with medium sensors.

The pontoon pier or ice surface [55] allows periodic maintenance, including maintenance necessitated by biological fouling of the portholes.

Let us briefly describe the data processing and particle classification procedure. This study presents the data obtained when measuring plankton in five water areas. Two points on Lake Baikal belong to the same geographical place, but to different seasons and configurations of moorage (Table 1). Every hour, the station records 20–45 digital holograms of the working volume of sea water with an interval of one second between frames. The sample volume is determined by the working volume (Table 1), which can be adjusted depending on the experimental conditions, for example, water turbidity. At typical flow velocities of 1–5 cm·s^{-1}, the flow of water through the sampling volume during the one-second interval between frames is comparable to the sampling volume itself; therefore, consecutive frames are treated as quasi-independent. This is an order-of-magnitude estimate, and the repeated recording of the same species at low flow velocities remains a source of additional uncertainty. Averaging across 20–45 holograms reduces this uncertainty but does not eliminate it. Hologram processing includes preprocessing, numerical reconstruction, and 2D display of a holographic image. 2D display of a holographic image

is the final flat image, which is collected from many fixed sections of the hologram and shows the focused (sharp) images of all particles of the studied volume on one plane. This significantly reduces the amount of data and processing time and serves as the initial image for automatic recognition and classification. A rectangle is described around a holographic image of a particle for automatic classification, and the key morphological features are the rectangle length H, the morphological parameter M, defined as the width–length ratio of the rectangle (W-H ratio), as well as the signs of the presence of outgrowths, i.e., any appendages, such as antennas, antennules or tail branches. Thus, the term "zooplankton" in this study refers to particles larger than 80 μm with the presence of outgrowths, which are divided by size and morphological parameter into Chaetognatha, Cladocera, Copepoda nauplii, Copepoda adult, Appendicularia, Rotifera and Other. Accuracy of classification, including false-positive and false-negative results, was confirmed in [58] and is about 60%.

Table 1. Sampling in the studied water areas. Station data sets marked with * are presented for the first time.

Water Body/Region	Station Coordinates	Monitoring Period	Segment Duration/Length	DHC Immersion Depth	Working Volume, dm³	Dominant Plankton Groups
Lake Bolshoye Yarovoye (Altai Territory)	N 52°55′01.00″ E 78°35′19.00″	27.06.2024–02.07.2024	3–6-day segments (Figures 3 and 4)	1 m from the bottom (bottom station)	0.037	Euryhaline *Artemia salina*; community is poor, no predators
Lake Baikal (Bolshiye Koty village), summer	N 51°53′57.12″ E 105°03′50.04″	03.08.2021–28.08.2021	3-day segments (Figure 5a,c)	2.5 m from the bottom (bottom station)	0.02	*Epischura baikalensis* (Copepoda), its nauplii, rotifers *Keratella cochlearis*, *Brachionus*
Lake Baikal (Bolshiye Koty village), winter	N 51°53′54.42″ E 105°03′53.46″	26.02.2022–24.03.2022 *	3-day segments (Figure 5b,d); 7-day segments were also used (Figure 6b,d,f)	10 m from ice	0.2	*Epischura baikalensis* (Copepoda), its nauplii, rotifers *Keratella cochlearis*, *Branchionus*
Barents Sea (Dalnye Zelentsy, Zelenetskaya Bay)	N 69°07′07.90″ E 36°04′10.00″	23.07.2022–24.09.2022	3-day segments; to resolve diagnostic rhythms increased to 5 days	4 m from the bottom (bottom station)	0.112	Large herbivorous copepods *Calanus finmarchicus*, *C. glacialis*, *C. hyperboreus*, *Metridia longa*; small copepods *Oithona similis*, *Pseudocalanus* spp., *Microcalanus* spp.; Copepoda dominates
Central Arctic (drifting station SP-42)	N 81°15′00.00″ E 141°15′00.00″	26.10.2024–18.03.2025 *	3-day segments	10 m	0.093	Arctic copepods: *Oithona similis*, *Oithona atlantica* (by number), *Calanus finmarchicus*, *Calanus glacialis* (by biomass); Copepoda dominates

Time series represent sequences of data measured at regular intervals that help to illustrate the dynamics of changes in values over time (Figure 3). Real-time data processing makes it possible to determine the amount of zooplankton in each hologram of the recording volume. Recalculation of this amount per unit volume allows the calculation of the average (averaged over several sequentially recorded holograms) concentration $\langle K_0(t_i) \rangle$ in the DHC working volume per hour of moorage. The Index 0 is used hereinafter to indicate background values, without active impact on zooplankton biocenosis.

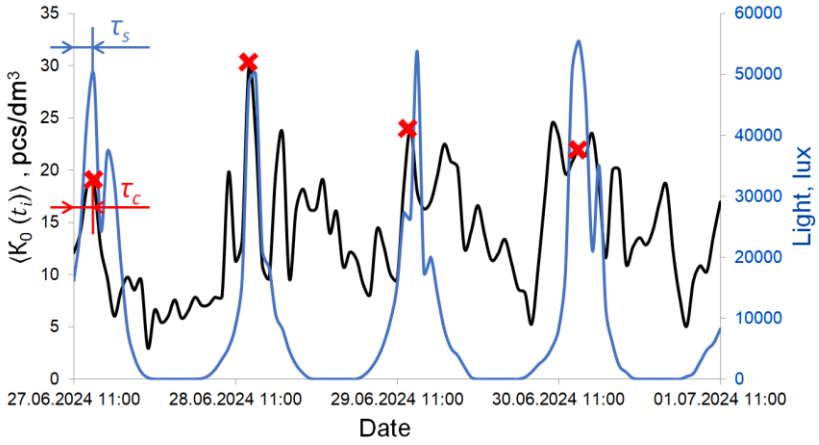


Figure 3. Time series (adapted from [57]) of euryhaline *Artemia salina* concentration (black line) from 27.06.24 to 02.07.24 at the bioindication station with the DHC, on Lake Bolshoye Yarovoye (N 52°55′1′′ E 78°35′19′′) against the background of the insolation graph (blue line). The position of the maximum (red X) of the upper illumination relative to the beginning of the time axis is indicated by τ_s (s-sun), the time shift of the initial phase for the circadian line—τ_c.

2.3. Spectral Model of Zooplankton Biocenosis

Explaining the causes and consequences of the variability of plankton concentrations at the point of the medium, we refer to the picture described in the Introduction, which is a standard record of the time series of zooplankton concentrations and its subsequent presentation as a Fourier series [54,56,59].

The number of analyzed medium factors is determined by the required modality of analysis, i.e., the time interval at which the series is considered. For diagnostic rhythms, these intervals or analyzed segments of the time series last several days.

The results discussed herein are related to recording the variability of zooplankton concentrations as a Fourier series with a finite number of harmonic components.

$$K_0(t_{ij}) \approx \langle K_{av}(j)\rangle + I_c{}^0(j)\cos\left(2\pi\frac{t_{ij}}{T_c}+\varphi_c(j)\right) + I_{dv}{}^0(j)cos\left(2\pi\frac{t_{ij}}{T_{dv}}+\varphi_{dv}(j)\right) + K_u(t_{ij}). \quad (1)$$

The harmonics presented in formula 1 reflect the rhythms of zooplankton biocenosis, which play the most critical role in the selected time interval $72\text{h} < 2T < 240\text{h}$, or within the corresponding duration of the segment of zooplankton concentration time series. In this case, the following designations apply:

- $\langle K_{av}(j)\rangle = \text{const} + I_{lf}{}^0(j)\cos\left(2\pi\frac{t_{ij}}{T_{lf}}+\varphi_{lf}(j)\right)$—mean daily concentration,
- $K_u(t_{ij}) = I_u{}^0(j)\cos\left(2\pi\frac{t_{ij}}{T_u}+\varphi_u(j)\right) + K_{hf}(t_{ij})$—ultradian component of diurnal band variability,
- $K_{hf}(t_{ij})$—high-frequency component of zooplankton concentration variability associated with peculiarities of taxonomic composition of biocenosis and particular movements of zooplankton individuals passing through the DHC working volume during hologram series recording,
- $I_k{}^0$—amplitude of the k rhythm in the Fourier spectrum of a number of zooplankton concentrations, pcs/dm^3,
- j—number of the time series segment,
- i—current intra-segment hour number,
- T_k—period of the k rhythm, hour,

- φ_k—initial phase of the k rhythm showing the shift of its maximum or harmonics in terms of expression (1) relative to 00 h of the j day, which is the beginning of the time coordinate t_{ij}, rad,
- indices k take the following values:
  - lf—low frequency,
  - c—circadian,
  - dv—semidiurnal variability,
  - u—ultradian.

A distinctive feature of diagnostic rhythms is their well-known period and driver. So, for the circadian rhythm, $T_c = 24$ h, where the driver is the sunrise, which initiates this rhythm every day with a period of 23–25 h [38]. The semidiurnal variability rhythm caused by nutrition processes is generated 2 times a day and therefore has period $T_{dv} = 12$ h [60]. Often this rhythm is called tidal [61], but tides are rather a driver of dv-rhythms, which initiates it with a period of 10–13 h in regions with semidiurnal tides and is synchronized by the rotation of the Earth.

In addition to the diagnostic rhythms, formula 1 includes lf- and u-rhythms, which are presented implicitly through the low-frequency and ultradian components of variability. Unlike diagnostic rhythms, lf- and u-rhythms cannot have a priori values of their periods. Therefore, the bioindication value of such rhythms is quite doubtful.

$\langle K_{av}(j)\rangle$ is a trend determined on the time interval taken for analysis, and is not a full constant throughout the time series or its segment, since there are environmental factors affecting this value, for example, rhythms associated with the relative position of the Moon and the Sun, the so-called syzygial tide and its alternation with quadrature, as well as low-frequency structuring rhythms [41]. However, the const value and harmonic description parameters $\langle K_{av}(j)\rangle$ can be determined based on the experimental data processing according to the least-squares method (LSM). The lf-component is treated as a local trend approximation, not as an established physical oscillation; its period is identified by the least-squares fitting within the segment and should be interpreted as an effective trend parameter.

$K_u(t_{ij})$ may have bioindicative applications [56], but due to high frequencies, small amplitudes and taxonomic specification, this variability component is not considered in this article. Moreover, we are trying to get rid of this component through averaging, the efficiency of which is assessed by controlling the strongest harmonic $K_u(t_{ij})$ of the u-rhythm.

For averaging, the original $K_0(t_{ij})$ time series is subject to window editing. As shown in [41], the 6 h window almost does not change the spectrum in the diagnostic frequency region, but eliminates high frequencies. This discrimination manifests itself in the fact that the window has an amplitude-frequency characteristic. Thus, [41] shows that the 6 h rectangular window weakens the dv-component almost 2 times more than the c-component, while the phase characteristic does not change.

Therefore, formula (1) can be rewritten as follows:

$$\langle K_0(t_{ij})\rangle_6 \approx \langle K_{av}(j)\rangle + I_c{}^0(j)\cos\left(2\pi\frac{t_{ij}}{T_c} + \varphi_c(j)\right) + I_{dv}{}^0(j)cos\left(2\pi\frac{t_{ij}}{T_{dv}} + \varphi_{dv}(j)\right), \quad (2)$$

where $\langle K_0(t_{ij})\rangle_6$ is defined as a smoothed time series of zooplankton concentrations obtained as a result of editing the initial series with a 6 h window. The $I_{dv}{}^0$ is indicated in this work without taking into account the transfer coefficient ~2. Note that this should be taken into account when comparing the values of the amplitudes of the rhythms given in the article and their contribution to the variability of non-averaged data.

Thus, having the a priori model (2), we have a tool for analytical alignment and analysis of experimental data.

We use the following to determine the parameters of rhythmic processes of zooplankton concentration change:

- smoothing procedures of the initial series $K_0(t_{ij})$ performed as window editing and spline interpolation of measurement data,
- spectral analysis by determining the Fourier coefficients for a series $\langle K_0(t_{ij})\rangle_6$—estimation of the contribution of components,
- optimal interpolation of a number of zooplankton concentrations according to formula (2) in order to analytically align experimental data, determine variability metrics and build a heuristic model,
- verification of the model with experimental data to determine discrepancies and quality metrics of the model.

It is formula (2), which is a Fourier series of zooplankton concentration that determines the bioindication potential of the behavioral activity of autochthonous zooplankton. In other words, the bioindication aspect of the behavioral patterns of biorhythms is revealed in the spectral harmonics of the Fourier series, just like the parameters of spectral lines in optics determine the composition of a substance [41].

The spectral analysis was performed on detrended data within a 3-day sliding window. The spectrum was estimated using the fast Fourier transform (FFT) method from a spline interpolated signal with an increase in the sampling frequency by 100 times.

The spacing of the frequency grid was 0.000139 Hz, but the actual resolution was limited by the window duration (theoretical limit $\Delta f \approx 1/72$ h) and further expanded by preliminary smoothing with a moving average (6 h window). The same 6 h moving average was used to suppress noise. The spectrum normalization was amplitude (units of plankton concentration).

Peak uncertainty was not estimated through confidence intervals of the spectrum, but by optimizing the harmonic phases using the Nelder-Mead method to minimize the root-mean-square-deviation (RMSD):

$$RMSD = \sqrt{\frac{1}{N}\sum_{i=1}^{N}|K_0(t_i) - \langle K_0(t_i)\rangle_6|^2},$$

where N—number of hourly observations in the segment (for a three-day window, N = 72). The relative model error was calculated as the ratio of the RMSD between the measured concentrations and those predicted by the model to the mean measured concentration over the analyzed segment:

$$\varepsilon = \frac{RMSD}{\langle K_0(t_i)\rangle} \times 100\%.$$

Since the parameters are estimated and evaluated on the same segment, RMSD characterizes the fitting error rather than the predictive performance.

2.4. Stress Tests

To test the hypothesis that diagnostic plankton rhythms have bioindicator properties during winter deployment on Lake Baikal, a localized, short-term, controlled "pollution" of the environment was performed. An indicator substance, NaCl (manufactured by BSK-sol Belgorod, Russia), was introduced from the surface for three days at a point of 1 m above the DHC working volume, in the form of a salt solution with a concentration of 300 g/L. The solution was supplied at a rate of 10 dm^3 per day, without generating turbulent flows. The beginning and end of the exposure were recorded using a water-conductivity sensor. These control observations showed that water conductivity changed by no more than 10% from its nominal value and returned to that value within 0.5 h after the

"pollution" ended. No independent replication was performed; therefore, the salt experiment is presented as a controlled perturbation case study, not as a replicated experiment.

During the Arctic drift of the ice-resistant platform SP-42, liquid organic waste generated during the flushing of onboard tanks of the research expedition vessel was selected as the pollutant for the same purpose. The waste consisted predominantly of fecal matter. To distinguish these particles from plankton during hologram processing, an additional taxon, Suspension, was added to the particle-recognition software (V1.2). The analysis of this taxon makes it possible to determine particle biomass from the DHC data. The minimum suspended-particle biomass concentration recorded in these experiments was approximately 200 mg/dm^3. A plume of particles settling from the discharge site to a depth of 10 m trails behind the ice floe for 3–5 days, increasing the biomass concentration by a factor of 3–8, depending on hydrological conditions and the discharge location. The time and location of each discharge were recorded in the vessel's logbook. The ability to measure organic matter together with plankton at the same temporal and spatial resolution is an important advantage of the method. Combining plankton and Suspension data collected in real time aboard the vessel makes it possible to objectively visualize the plankton response to the introduction of a pollutant.

Thus, both stress tests represent controlled impact conducted for experimental purposes as part of a field study.

3. Results of Field Experiments and Data Processing

When choosing locations for the station, we relied on different climatic conditions and different taxonomic compositions of zooplankton to be able to demonstrate the versatility of the spectral approach to data interpretation and processing, despite various regional factors.

3.1. Analysis of the Mesoscale Rhythmicity of Artemia salina at Lake Bolshoye Yarovoye, Altai Krai, Russia

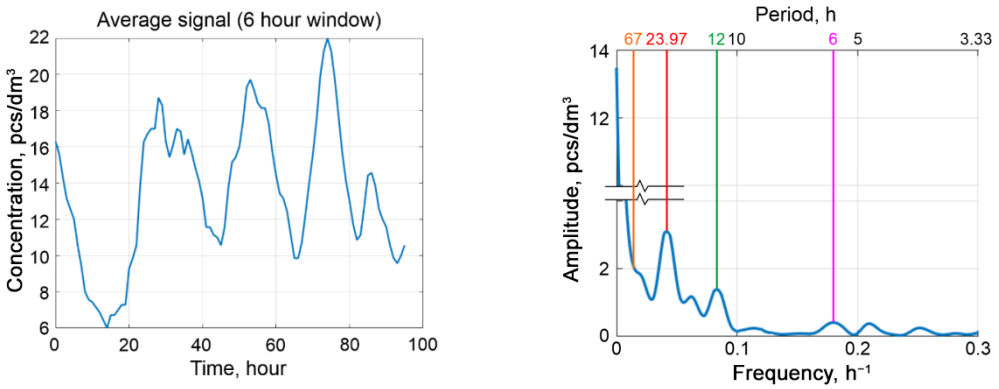
Lake Bolshoye Yarovoye is an inland salty water body in the middle latitudes. Zooplankton biocenosis is very poor, represented by euryhaline *Artemia salina*, without predators. The daily insolation mode is quite normal, characteristic of middle latitudes. Measurements were performed in summer with the maximum duration of daylight hours. The DHC was located at a fixed 1 m distance from the bottom (Table 1).

The graph of the time series of plankton concentrations shown in Figure 3 reflects the variability rhythm, which almost coincides with the dynamics of variability of the upper illumination caused by solar activity.

The maxima of concentrations (marked with a red cross in Figure 3) are observed at times when the Sun was at its zenith (~12 p.m.). The shift of the solar insolation maximum relative to the beginning of the session is $\tau_s \approx 4$ h.

The processing of the original variability graph with a 6 h window made it possible to eliminate high-frequency fluctuations and outliers from the initial data series, perform spline interpolation of the experimental data and construct the amplitude spectrum using a Fourier transform. In this case, the window size does not have a strong effect on the characteristic lines [41]. The result is shown in Figure 4.

https://doi.org/10.3390/w18232985



(**a**) (**b**)

Figure 4. Time series segment of zooplankton concentrations from Figure 3, smoothed by a 6 h window for subsequent Fourier analysis—(**a**). Readings of the measured concentration values averaged over 120 holograms (taking into account window processing). The amplitude Fourier spectrum of this segment—(**b**). The rhythms are represented by colored vertical lines: orange—low-frequency or lf-line, red—c-line of circadian rhythm, green—dv-line of semidiurnal variability rhythm, purple—u-line of ultradian rhythm. The amplitudes of the rhythms are given without taking into account the transmission coefficient for the 6 h window.

The spectral representation of the segment (Figure 4b) demonstrates the presence of three active pronounced lines: a low-frequency component (T_{av} = 67 h), a circadian line ($T_c = 24$ h), and a semidiurnal variability line ($T_{dv} = 12$ h). In other words, the spectrum is quite linear and it is fair to use the model described by formula 2 to simulate a number of zooplankton concentrations, since the amplitudes of ultradian rhythms after window editing are negligible, and the tidal rhythm is not separately observed or is within the dv-rhythm line.

Table 2 shows model parameters for a number of zooplankton concentrations after 6 h window editing to reduce the impact of high-frequency components and outliers. The formula $\tau_c = -\frac{\varphi \cdot T}{2\pi}$ is adopted to calculate the time interpretation of τ [hour] of phase φ [rad] of the rhythm with the period T [hour].

Table 2. Parameters of the model variability of *Artemia salina* concentrations on Lake Bolshoye Yarovoye.

Line	Period T_k, h	Amplitude I_k^0 for Average Signal (6 h Window), pcs/dm³	Initial Phase φ, rad/Time of Maximum τ_c, Hour for Cosine Representation
Constant	-	13	-
Low-frequency component, lf	67	2	-
Circadian, c	23.97	3.25	−1.15/−4.2
Tidal	12.8	0.61	1.24/2.53
Semidiurnal variability, dv	12	1.44	−1.59/−3.26
Ultradian, u	8.7	0.25	−6.72/−9.3

The phase data given in the last column of Table 2 show the variability of the initial phase of the rhythms present in the spectrum in connection with the measurement time reference at the station. For the circadian line, $\varphi_c = -1.15$ rad, which corresponds to $\tau_c = -4.2$ h, i.e., the concentration maximum occured approximately 4.2 h after the beginning of the day. This value is close to the solar insolation maximum $\tau_s \approx 4$ h in Figure 3, suggesting that sunlight initiates the rise in zooplankton to the upper layers.

Of all the presented lines, only the circadian, ultradian and semidiurnal variability lines are associated with the life cycle, primarily with zooplankton nutrition, and hence, they have bioindication informativity. The low-frequency component refers to structuring rhythms associated with turbulence, and the tidal rhythm refers to tidal processes, which are almost not observed in this water area. If for circadian and ultradian rhythms the synchronizing reasons are quite obvious—the Sun, for low-frequency—a wind direction change, then the connection of semidiurnal variability with tides in this water area is not so obvious. Since the c-line (circadian) significantly exceeds all other lines in amplitude, this determines its dominant value for bioindication.

3.2. Features of Mesoscale Plankton Rhythmicity at the Bioindication Station at Lake Baikal (Bolshiye Koty Settlement) in Summer and Winter Experiments

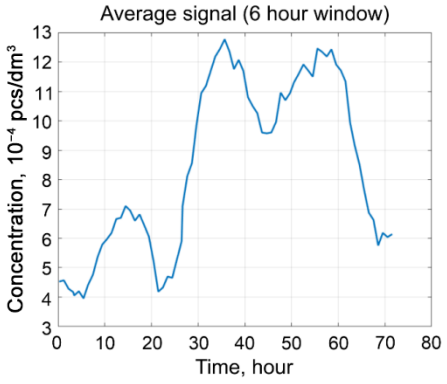
Lake Baikal is a lake of tectonic origin located in the southern part of Eastern Siberia, the deepest lake on Earth and the largest natural fresh water reservoir.

The daily insolation mode is normal, characteristic of middle latitudes. The unique nature of Lake Baikal ecosystem is the purity of its water, which is maintained by endemic organisms [62].

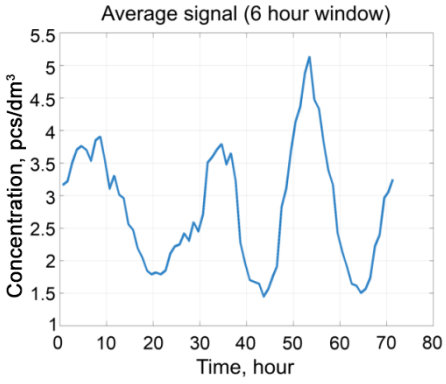
Furthermore, the pelagic community of Lake Baikal is naturally quite poor and therefore may serve as a good model to study the behavior of zooplankton [9,10,25,63]. *Epischura baikalensis* (Copepoda), its nauplii and rotifers *Keratella cochieals*, *Branchionus* dominate year-round in the coastal zone of the lake. The paper [12] demonstrates that it is these organisms that act as true indicators of processes in Lake Baikal. Moreover, in laboratory conditions it was shown that the lake endemics have bioindication dominance compared to *Dafnia magna* traditionally used for this purpose [64]. Since *Daphnia magna* is significantly more resistant to changes in the natural environment, the daphnia test is not sensitive enough to assess the ecological cleanliness of Lake Baikal.

During the summer measurements conducted on Lake Baikal, the DHC was positioned at the bottom of the station, maintained at a constant distance of 2.5 m above the lakebed. During winter measurements on this lake, the DHC was lowered from the ice to a depth of 10 m (Table 1).

The typical data on zooplankton concentration measurements characteristic of the tranquil conditions of Lake Baikal are presented as three-day segments of the time series. Figure 5a illustrates such data for the summer period of 2021, while Figure 5b shows the corresponding data for the winter period of 2022.



(**a**)



(**b**)

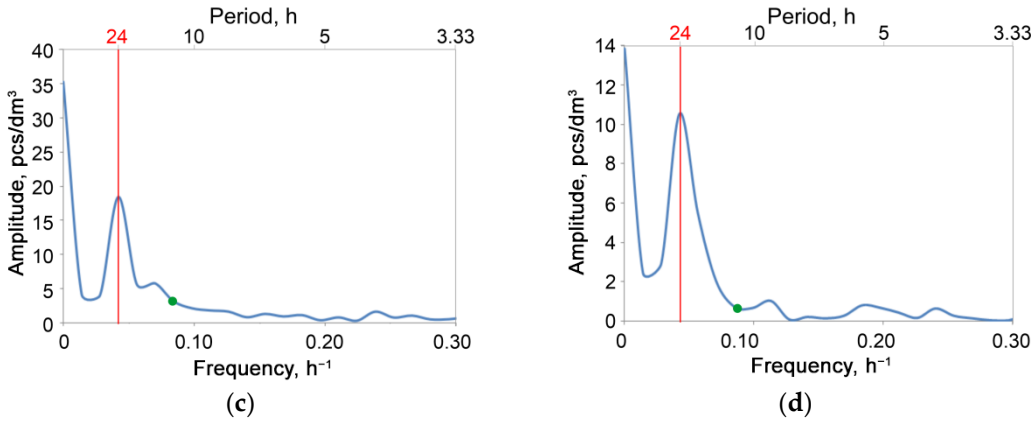


Figure 5. Typical three-day segments of zooplankton concentration series recorded on Lake Baikal (after treatment with a 6 h window) in summer (25.08.2021–28.08.2021)—(**a**) and winter (10.03.2022–13.03.2022)—(**b**) and respectively their Fourier spectra (**c**,**d**). The red line marks the c-rhythm, while the green dot—the dv-rhythm. The amplitudes of the rhythms are given without taking into account the transmission coefficient for the 6 h window.

The spectral analysis of these three-day segments indicates a relatively simple rhythmic pattern, shown in Figure 5c,d for the summer and winter periods, respectively. This rhythmicity is overwhelmingly dominated by the circadian cycle of zooplankton concentrations. The influence of the dv-rhythm is almost negligible, contributing minimally to the overall pattern. Given that the tidal range in Lake Baikal is insignificant—tidal elevations do not exceed 3 cm [65,66]—tidal rhythms are effectively absent from the observed data.

There are two differences between the summer and winter spectra for Lake Baikal, namely:

- the amplitude of the circadian rhythm line in summer is 2 times higher than the amplitude in winter,
- the low-frequency part of the spectrum for summer zooplankton is more powerful, which indicates a pronounced s-rhythm due to regional factors.

Given that the dominant spectral line of the circadian rhythm is unambiguously interpreted, let us analyze potential causes for the pronounced s-rhythm.

The primary seasonal factor influencing the inhomogeneity in zooplankton distribution is the thermal regime of the lake, which depends not only on heat exchange with the overlying atmospheric air but also on wind- and wave-induced mixing, currents, and other dynamic phenomena [67].

This specificity can significantly affect the spectra of zooplankton concentrations, either indirectly through the impact of temperature variations or directly via advection and diffusion of zooplankton organisms. The surface and internal waves generated by the movement of air and water masses also play a crucial role in this process [46].

Furthermore, frequent changes in wind conditions predominantly determine the regional characteristics of Lake Baikal's zooplankton spectra by influencing the amplitude of s-rhythms.

Like any s-rhythm, high-frequency s-rhythms are associated with the three-dimensional structure of turbulent energy-bearing vortices and their variability caused by changes in boundary conditions, particularly water level fluctuations. The frequency of these changes dictates the frequency of s-rhythms [41], thereby shaping the regional specifics in the structure of environmental influencing factors [65], as reflected in the segments in Figure 6 recorded during periods of heightened wind activity.

15 August 2021,
s-rhythm summer

12 March 2022,
s-rhythm, winter

15 March 2022,
Impact,
winter

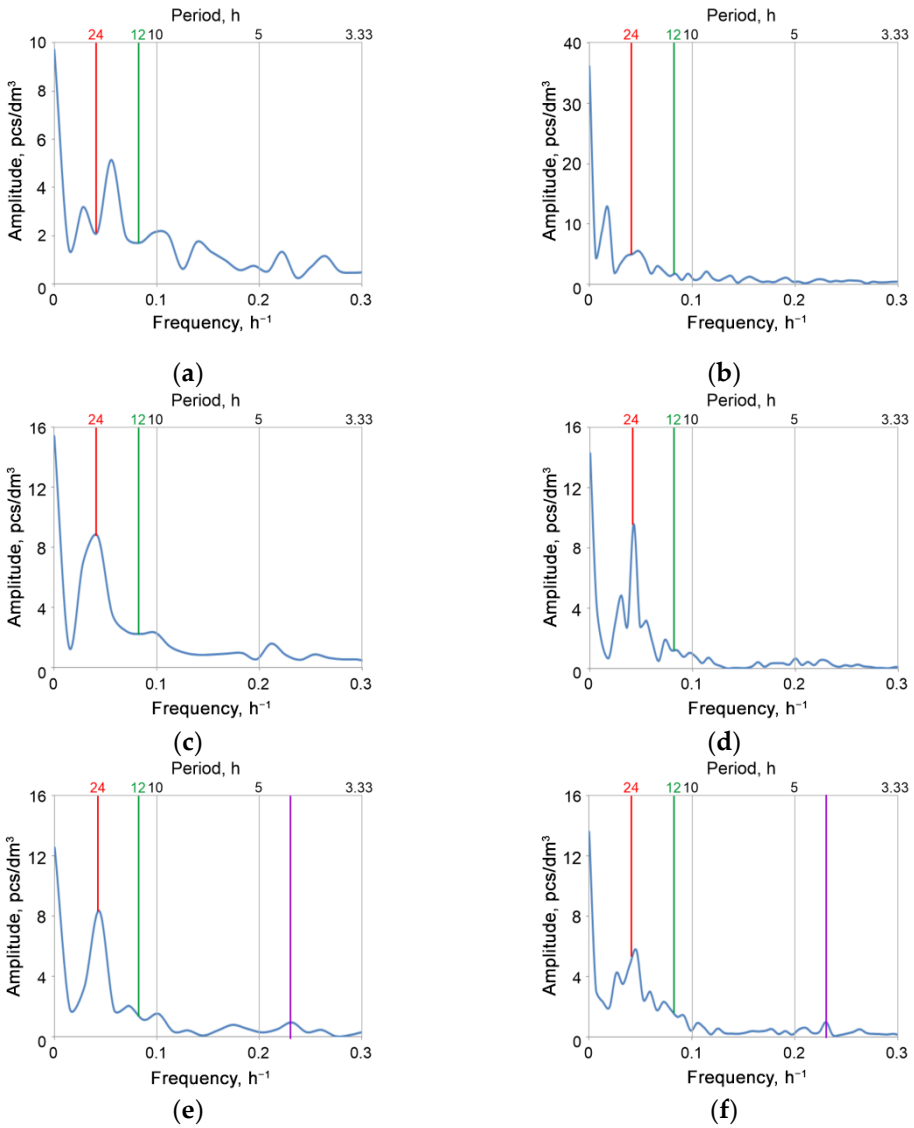


Figure 6. Increase in spectral resolution with the increase in the time-series concentration segment ((**a**,**c**,**e**)—three days, (**b**,**d**,**f**)—seven days) to determine circadian rhythm parameters during the action of s-rhythms within the mesoscale modality—(**a**–**d**), and authorized saline exposure—(**e**,**f**) The red line indicates the c-line, the green line—the dv-line, the lilac line—the u-line. The amplitudes of the rhythms are given without taking into account the transmission coefficient for the 6 h window.

The diverse periodicity, recurrence, and energy of these heterogeneous factors lead to the formation of internal waves within the water body as a result of their interactions. These internal waves influence vertical and horizontal exchange processes, which are vital for hydrobiology, hydrochemistry, and overall lake ecology [42–44].

Modeling the processes leading to internal wave formation in Lake Baikal indicates that large-scale vortex systems develop even in the central and northern parts of the lake under conditions of homogeneous fluid density.

The high-frequency s-rhythms observed in our experiments on zooplankton, utilizing underwater holography, align well with this interpretation and offer an explanation for the emergence of rhythms that compete in amplitude with the circadian rhythms. However, since these s-rhythms obstructed the detection of the circadian rhythm and could potentially lead to an unfounded conclusion regarding the disappearance of the circadian cycle (bioindicator collapse), additional measurements and an extension of the time series segment were necessary. Specifically, the segment length was increased from three days (Figure 6a,c) to seven days (Figure 6b,d). The poor spectral resolution of the c-

line within three-day intervals results in significant broadening, causing the spectral contour to encompass both the primary (informational) circadian line and lateral s-lines, which lack bioinformative status. Over seven-day segments, the c-line becomes sufficiently pronounced with improved spectral resolution.

During the period of authorized influence, namely, the application of a pollutant—salt solution—spectrum of the circadian rhythm shifted within the three-day segments, particularly in the winter series. These spectral transformations are illustrated in Figure 6e,f. The spectra of the seven-day segments reveal the formation of additional lines, displaced from the circadian rhythm into the high-frequency domain, indicating the emergence of significant dv- and ultradian rhythms despite smoothing over six hours.

Consequently, the practical distinction between the spectral signatures of zooplankton concentration variability associated with s-rhythms and those during pollutant introduction resides in the amplification of high-frequency components. This indicates that, rather than engaging in regular activity patterns, the zooplankton exhibit irregular, disordered activities during the disturbance period.

This trend is well illustrated by the graph in Figure 7, where the disarray of habitual rhythms manifests as a more than twofold increase in the RMSD of the original data during the pollutant application period.

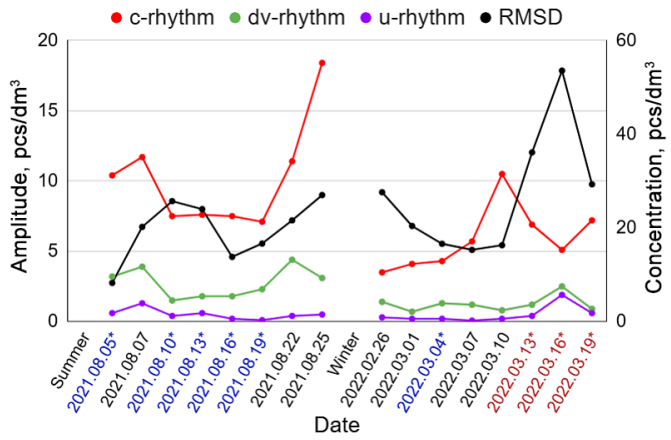


Figure 7. Parameters of diagnostic rhythms for segments of the recorded time series of zooplankton concentration, the blue asterisk (*) marks a day for which spectral parameters were determined for seven-day segments during periods of wind activity, the red asterisk (*)—parameters were determined for seven-day segments during controlled application of the pollutant. The amplitudes of the rhythms are given without taking into account the transmission coefficient for the 6 h window.

The primary conclusion is that, despite the predominance of the circadian line, the biorhythmological model of biocenosis—considering internal wave phenomena of the water body as a regional environmental factor—must incorporate dv-, lf-, and u-rhythms as essential and auxiliary diagnostic components to accurately describe such spectral signatures.

3.3. Features of Mesoscale Plankton Rhythmicity at the Bioindication Station in the Barents Sea (Dalnye Zelentsy) Under Tidal Variability

Zelenetskaya Bay is a shallow coastal inlet located on the eastern Murmansk coast (Eastern Murmansk). The bay's mouth is oriented towards the north-northeast. Five small islands situated at the mouth serve to protect it from open sea waves. During syzygial tides, some of these islands become connected by isthmuses. The total water area of the bay (excluding the islands) is slightly over 2 km^2. The sampling scheme is presented in Table 1.

The seabed terrain within the bay is complex; depths in the western part, which is the deepest area, do not exceed 11 m during low tide. Most of the bay's area has depths less than 7 m. In both the eastern and western parts, there are small depressions reaching depths of 15–18 m, imparting distinctive features to an otherwise relatively homogeneous hydrological regime. In the open sea, to the west of the bay, a trough extending with depths exceeding 200 m approaches the area. Along this trough, a branch of the warm Murmansk coastal current influences the bay's hydrology [68,69].

Hydrometeorological factors affecting the oceanographic characteristics of the bay include wind and air temperature regimes. The prevailing winds in the bay are south-western (recurrence approximately 30%), north-western (15%), and western (13%). Winds from other directions occur less than 10% of the time [70].

These local features, similar to those observed at Lake Baikal, create conditions for the appearance of internal waves in the water body. These internal waves act as regional environmental factors that influence the rhythmicity of zooplankton populations.

It is generally accepted that key zooplankton species in the Barents Sea include large herbivorous copepods such as *Calanus finmarchicus, C. glacialis, C. hyperboreus*, and *Metridia longa*. During the spring-summer period, these species comprise up to 90% of the total mesozooplankton biomass. Among smaller copepods (body size ≤ 1 mm), *Oithona similis*, *Pseudocalanus* spp., and *Microcalanus* spp. dominate numerically [71].

The near-complete isolation of the water body from the open sea creates unique conditions that contribute to a certain divergence in the biocenosis of the bay from the Barents Sea pelagic ecosystem. Specifically, through selection and sampling via net catching it has been established that the average concentrations of zooplankton vary from 5.270 to 21.277 pcs/m^3, depending on the location and time of sampling. The mean concentration stands at 11.060 ± 1.811 pcs/m^3. Copepoda constitute the dominant taxon both in terms of biomass and concentration. In terms of species composition, *Oithona similis* and Copepoda nauplii are predominant.

The pattern of daily insolation is typical for high latitudes, namely, the polar day during mid-summer and the polar night during mid-winter. Consequently, twice annually, the zooplankton rhythm is not driven by the daily cycle of solar illumination, which leads to the expectation that a significant role is played by its second harmonic—the dv-rhythm—maintained by tidal regimes. The tidal cycle here is semi-diurnal, featuring a high amplitude: the difference in water level between high and low tide during syzygial tide reaches 4–4.2 m (this is particularly relevant in the context of discussed tidal rhythms), while in quadrature, it is approximately 2 m.

The pronounced amplitude of the tide at this station facilitates the study of the t-rhythm (tidal rhythm). Tidal processes can be visualized through a series of measurements of water depth at the station, obtained via pressure sensors. It should be noted that bioindication equipment, together with a submersible digital holographic camera, was mounted on a bottom station at a fixed distance from the seabed. The tidal periodicities, as depicted in the pressure graph (Figure 8a), are characterized by a period T_t (tides) modulated by an external frequency. This modulation manifests as beat phenomena with period T_s (spring tides) and is linked to astronomical factors, specifically the relative positions of the Moon, Earth, and Sun [72].

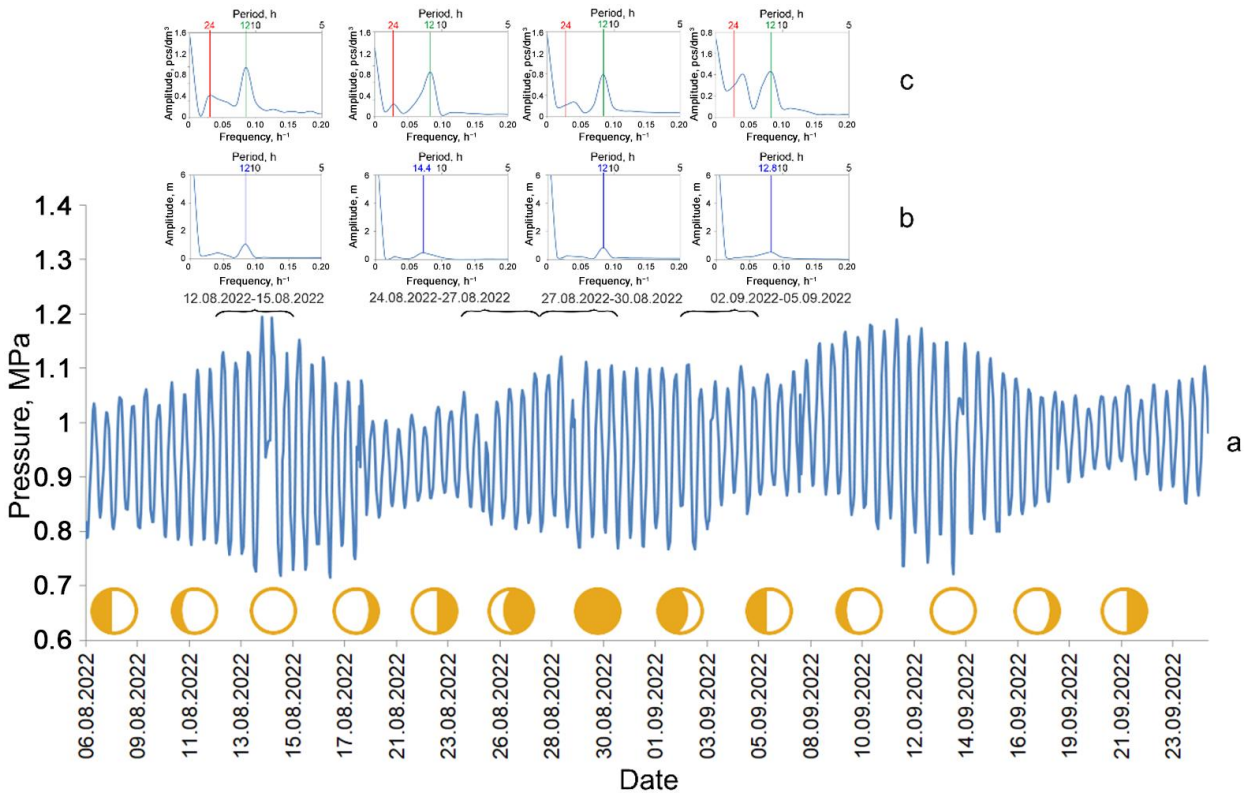


Figure 8. Time series of hydrostatic pressure measurements at the station in Dalnye Zelentsy (N 69°7′7.9″ E 36°4′10″)—(**a**). Spectra of hydrostatic pressure variability at the DHC site within the mesoscale modality (three-day segments). The blue vertical line shows the position of the tidal rhythm line with duration T_t in a given time interval—(**b**). Variability spectra of zooplankton concentrations—(**c**) at the DHC site within the mesoscale modality (three-day segments, in the same periods as in (**b**)). The red line—c-rhythm (T_c = 24 h), green line—dv-rhythm (T_{dv} = 12 h). The blue vertical line shows the position of the tidal rhythm line with duration T_t. Pictograms ● and ○ mean full moon and new moon, respectively. The amplitudes of the rhythms are given without taking into account the transmission coefficient for the 6 h window.

By conducting the Fourier analysis of segments of the pressure time series, it has been established that the frequency of the tides, which determines the tidal rhythm, is not a constant value. Specifically, for the location of the bioindication station and the analyzed zooplankton concentration variability series, the period of the tidal rhythm varies within the range of 12 to 14.4 h. The average value of this period is calculated as T_t =13.2 h. Examples of the spectra of the depth value segments at the station location, determined via pressure sensors, are shown in Figure 8b. The tidal rhythm line is marked with a blue line, with period values indicated on the time axis.

In developing a heuristic model of zooplankton concentration variability—which was measured using the DHC—it is necessary to evaluate the extent to which the tidal rhythm can be traced in a critical component of the spectrum, namely, the dv-line. This analysis aims to determine whether variations in T_t within the specified range influence T_{dv}. By comparing Figure 8b,c, we can conclude that the position of the dv-line is invariant to the observed fluctuations of the tide period (12–14.4 h).

The results of the Fourier analysis of three-day segments, shown in Figure 8c, support the following conclusions:

- The dv-rhythm in this water area not only competes with the circadian rhythm in terms of significance but slightly exceeds it during certain periods. This emphasizes

the importance of considering this rhythm alongside the circadian rhythm in models of zooplankton concentration variability.

- Variations in the parameters of the tidal rhythm, which drives the dv-rhythm, do not affect the position of the dv-line within the spectrum of zooplankton concentration variability. This suggests that the dv-rhythm has endogenous synchronization, similar to the circadian rhythm. Consequently, in the variability model, $T_{dv} = 12$ h can be considered an a priori fixed parameter, with the tidal rhythm acting as its driver. Therefore, it is unnecessary to explicitly incorporate the tidal period into the model.

Accounting for the influence of syzygial tides within the model proves to be somewhat more complex, given that their manifestations exist in a different modality. Specifically, detecting rhythmicity associated with lunar phase transitions requires a data series significantly longer than three days. As demonstrated in [41], the trend related to syzygial phenomena can be identified through windowed processing using a 72 h window. Importantly, it can only be constructed after the completion of all measurements, thereby delaying prediction indefinitely.

A more straightforward correction aimed at enhancing the resolution of diagnostic spectral lines—namely, the circadian and dv-lines—entails subtracting a locally known low-frequency trend from the original data segment. A heuristic approach to determining the parameters of low-frequency rhythms can be based on Fourier decomposition, leading to the extraction of a differenced series devoid of low-frequency components, including syzygial rhythms. The result of such processing is illustrated in Figure 9.

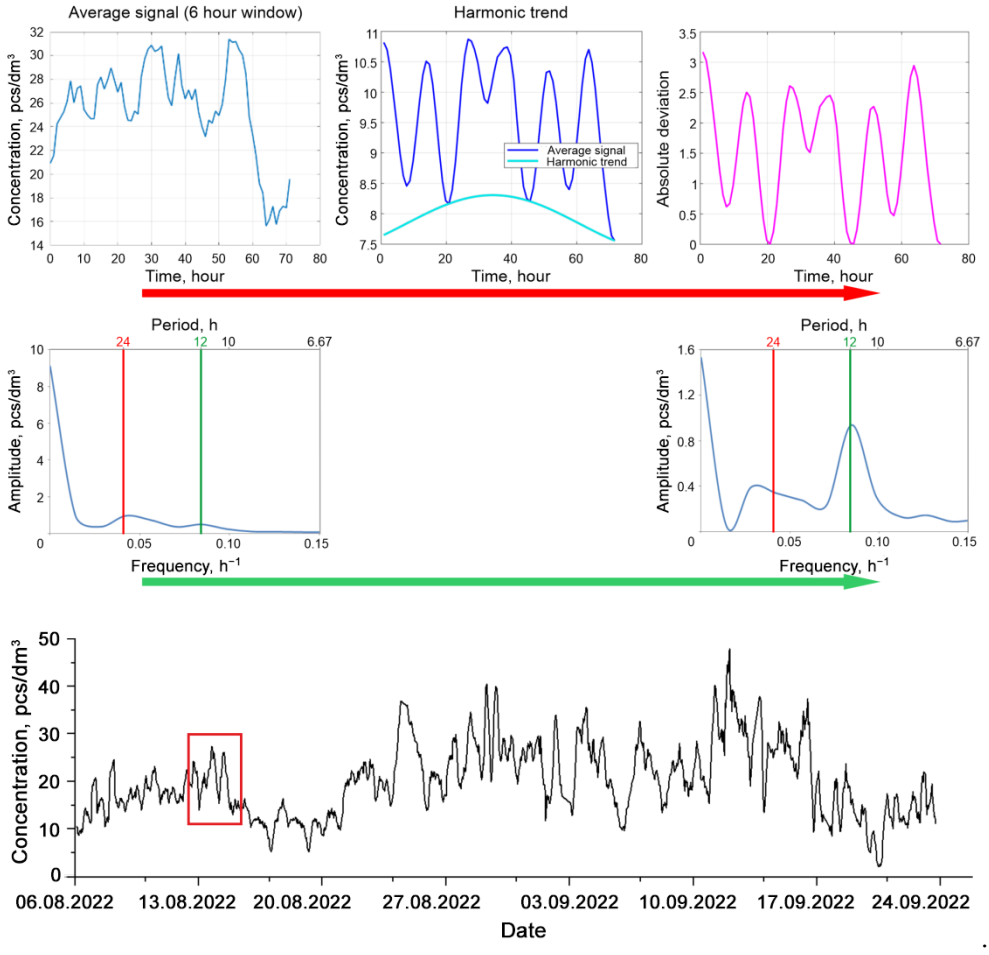


Figure 9. Correction of monitoring data with local trend correction in the segment 12–15 August 2022 of the initial time series of zooplankton concentrations (lower graph). Above—sequential modification of the time series segment. The red arrow shows the transition from these concentration

readings to a modified spline interpolated signal to form intermediate samples through harmonic trend parameters (red line). The green arrow in the middle line shows the transformation of the spectrum. The amplitudes of the rhythms are given without taking into account the transmission coefficient for the 6 h window.

The specific location of the station in Dalniye Zelentsy is characterized by its high northern latitude, and measurements conducted during the polar day. However, with the transition to polar night, the duration of nighttime increased rapidly from day to day. Consequently, the phase of the solar rhythm τ_s was continually shifting, making it non-trivial to assess the stability of the circadian rhythm under the conditions of the impending polar night and strong high-frequency s-rhythms. To address this, we increased the segment length of the time series to five days to better resolve diagnostic lines related to both circadian and semidiurnal variability. Representative results for key segments are shown in Figure 8c.

The parameters of the diagnostic lines used to construct the variability model of zooplankton concentrations are summarized in Table 3.

Table 3. Parameters of diagnostic lines and model line of low-frequency rhythm at the DHC site within mesoscale modality (five-day segments, during the same periods as in Figure 8c). The amplitudes of the rhythms are given without taking into account the transmission coefficient for the 6 h window.

Date	c-Rhythm			dv-Rhythm			lf-Rhythm		
	Amplitude, pcs/dm³	Phase, rad	Line Width at Half Height, 1/h	Amplitude, pcs/dm³	Phase, rad	Line Width at Half Height, 1/h	Amplitude, pcs/dm³	Phase, rad	Period, Hour
14 August 22	0.22	3.12	Poor resolution	0.77	4.56	0.01	0.05	−1.6	180
28 August 22	0.18	−4.0		0.71	−1.4	0.015	0.48	−0.3	200
01 August 22	0.15	−3.5		0.74	4.37	0.014	0.32	−2.36	175
04 August 22	0.09	4.1		0.35	1.47	0.02	0	-	-

From these considerations, we conclude that under conditions of highly variable solar climate at high latitudes, with a diverse biocenosis, the dv-line provides more valuable information for bioindication than the circadian line. The dv-rhythm line, while endogenous for coastal zooplankton, exhibits an amplitude 3–5 times greater than that of the c-line. Moreover, during tidal activity or factors related to seasonal influences, such as temperature drift in Lake Baikal, crucial correction involves removing the local trend or low-frequency variability, which amplitude can be comparable to that of the diagnostic dv-line.

3.4. Testing the Spectral Analysis Algorithm for Time Series Data of Polar Zooplankton Concentrations in the Arctic Ocean (AO), Recorded During Drift at the Polar Station SP-42

The Central Arctic Basin is a unique natural region characterized by distinctive physico-geographical and climatic conditions. The sea ice cover and prolonged polar night significantly restrict the period conducive to biological productivity, resulting in marine ecosystems that are both qualitatively and quantitatively impoverished. Consequently, these ecosystems exhibit high sensitivity and vulnerability to external impacts [73]. The drift sampling scheme is presented in Table 1.

The species composition of zooplankton in this region is represented primarily by a community of Arctic copepods, including small-sized filter feeders such as *Oithona similis* and *Oithona atlantica* (by abundance), as well as larger predatory copepods like *Calanus finmarchicus* and *Calanus glacialis* (by biomass). Therefore, the Copepoda taxon is

dominant, and the rhythmicity of zooplankton concentrations is primarily determined by the biological activity of these copepod species. Given the aforementioned sensitivity, an especially pertinent factor is the degree of upper illumination, which acts as a stimulus for circadian rhythms, disappearing and reemerging during the transition from polar day to polar night for deeper species.

The objective of the study presented in this section is to develop an understanding of the mesoscale rhythmicity structure of zooplankton concentrations within the Arctic Basin to evaluate the bioindication potential of spectral metrics associated with circadian rhythms.

Figure 10 illustrates segments of the observation series across the autumn-winter-spring seasons, demonstrating the transformation of variability signatures and their spectra during the transition from polar day to polar night and vice versa.

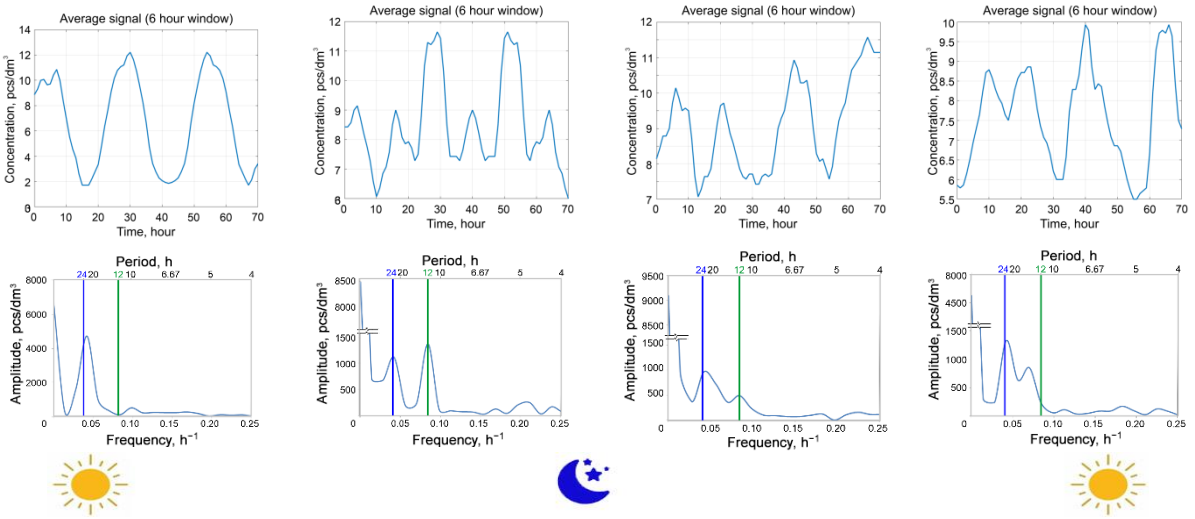


Figure 10. Transformation of signatures of mesoscale variability spectra during transition from polar day to night and vice versa. The amplitudes of the rhythms are given without taking into account the transmission coefficient for the 6 h window. Pictograms and refer to polar day and polar night, respectively.

Figure 11 gives an understanding of the role of standard diagnostic rhythms in the variability of zooplankton concentrations at high latitudes. It presents graphs depicting changes in the amplitudes of diagnostic rhythms. The dynamics shown in these graphs indicate a substantial reduction in the contribution of the circadian rhythm to variability in zooplankton concentration series following the onset of polar night.

https://doi.org/10.3390/w18232985

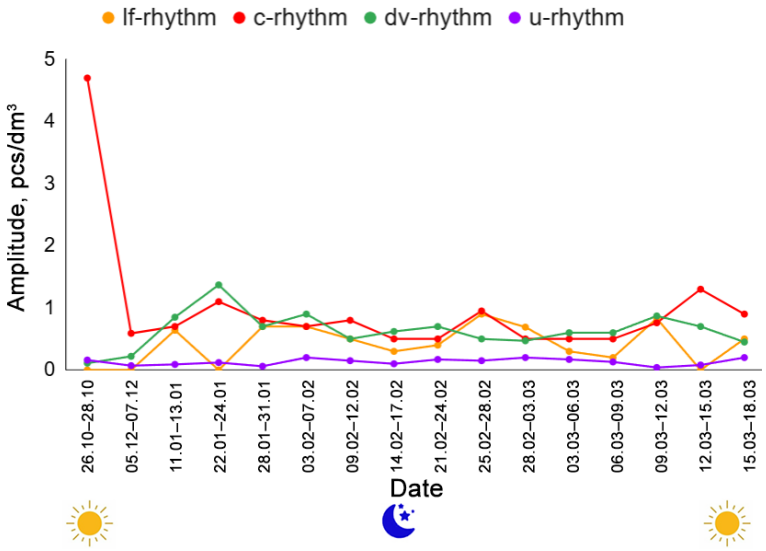


Figure 11. Variation in the amplitudes of diagnostic rhythms (standard series) in the spectrum of variability of zooplankton concentrations during the polar night. Pictograms and refer to polar day and polar night, respectively. The amplitudes of the rhythms are given without taking into account the transmission coefficient for the 6 h window.

The conclusion herein emphasizes that the bioindication studies must account for both diagnostic rhythms, given the exchange of energy fluctuations between them. This understanding leads to the concept of a three-frequency model of stationary variability, which incorporates the lf-rhythm—an element that does not impose a direct bioindication load but is essential as a parameter defining the trend across the segment length.

As with previous experiments, the lf-rhythm is associated with the influence of changing turbulent modes. In this context, the scale of variability during the drift process is determined by the alteration of course and temperature deviations. However, within the localized three-day model, these factors collectively constitute a single low-frequency harmonic.

Figure 12 illustrates graphs representing the error of the model dependent on moorage time with segments arranged along a common temporal axis.

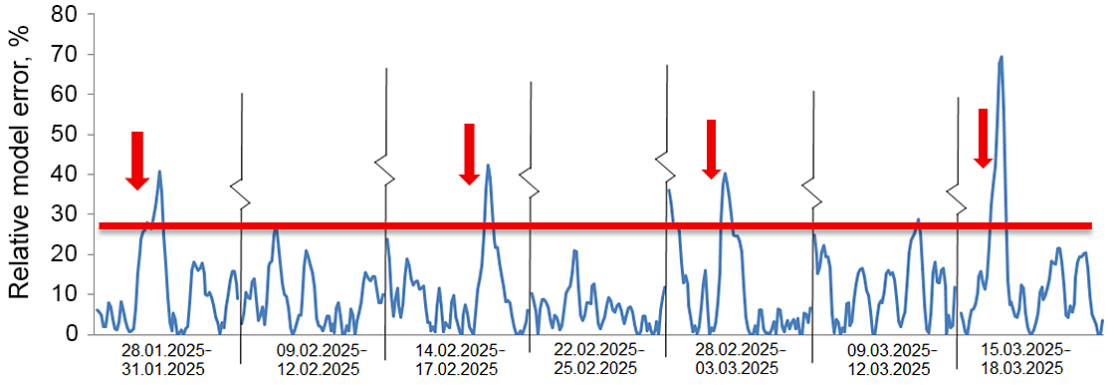


Figure 12. Variability of model error by moorage dates. The red arrows mark the time of organic waste discharge recorded by the vessel time and confirmed by the Suspension taxon analysis. 27% (marked with a red line) is an estimate of experimental error (image-classification error + sampling variability).

The overlay of the model's error with the graph of pollutant release from the SP-42 (marked by a red arrow in Figure 12) allows visualization of the plankton response to

pollutant influx as deviations from the rhythmic pattern. Such rhythmic disturbances are identified when the model's error exceeds the experimental data error threshold, indicated in the figure by a red line.

4. Discussion

The results of fieldwork are summarized in Table 4 for further comprehensive analysis.

Table 4. Objectives of the study and results of field experiments.

Water Area (Number of Analyzed Time Segments)	Features of the Water Area in the Context of the Study	Diagnostic Lines	Low Frequency Rhythm	Hypothesis Underlying the Results
Lake Bolshoye Yarovoye (1)	Inland saline water body of medium latitudes. The plankton community is very poor, represented by euryhaline *Artemia salina*, predators are not found. The daily insolation mode is normal, characteristic of middle latitudes. Measurements were made in summer at maximum daylight hours. DHC was placed at a fixed 1 m distance from the bottom.	Spectral line structure; presence of diagnostic rhythms: c-line dominates (24 h), synchronized with upper illumination, dv-line is weak (12 h), t-line is absent. C-line amplitude significantly exceeds the other lines.	lf-rhythm is pronounced (T ≈ 67 h), associated with turbulence and structuring processes.	Hypothesis 1 (spectral line structure and systematic component in the variability of concentrations); hypothesis 2 (sufficiency of 3-day segments and three rhythms to describe the systematic component of variability).
Lake Baikal (45)	Tectonic lake in the southern part of Eastern Siberia. The plankton community is naturally poor: *Epischura baikalensis* (Copepoda) dominates, its nauplii and rotifers *Keratella cochlearis*, *Brachionus*. The daily insolation mode is normal, characteristic of middle latitudes. In summer, the DHC was fixed at a bottom station 2.5 m above the bottom; in winter—lowered from the ice to a depth of 10 m.	Spectral line structure; presence of diagnostic rhythms: c-line dominates (24 h), dv-line (12 h) is minimal, t-line is absent. In summer, the amplitude of the circadian line is 2 times higher than in winter.	lf-rhythm is pronounced, especially in summer; associated with regional factors—wind and wave action, currents, internal waves, thermal lake regime. Lf-rhythms may compete in amplitude with c-rhythms, which requires an increase in segment length from 3 to 7 days	Hypothesis 1 (spectral line structure and systematic component); hypothesis 2 (sufficiency of 3–7 day segments and three lines to describe the systematic component of variability, of which two are diagnostic); hypothesis 3 (abnormal structure of diagnostic rhythms indicates the environmental degradation of biocenosis, mathematical techniques—subtraction of a local lf-trend—allow separating non-system variability caused by a regional factor).
Zelenetskaya Bay (22)	Shallow coastal bay on the eastern Murmansk Coast. Key zooplankton species: large herbivorous copepods *Calanus finmarchicus*, *C.*	Spectral line structure; presence of diagnostic rhythms: dv-rhythm (12 h) competes with c-	lf-rhythm is pronounced, associated with the change in turbulent structures	Hypothesis 2 (sufficiency of 3–5 day segments and a limited and a priori known set of diagnostic rhythms); hypothesis 3

	glacialis, *C. hyperboreus*, *Metridia longa*; small copepods *Oithona similis*, *Pseudocalanus* spp., *Microcalanus* spp. Copepoda dominate. Insolation mode is typical for polar latitudes. In autumn, the DHC is placed at the bottom station 4 m above the bottom.	rhythm (24 h) in importance and even exceeds it in certain periods. The position of the dv-rhythm line is invariant with respect to the observed fluctuations in the tidal period (12–14.4 h).	caused by water area hydrology. Local trend correction and segment growth up to 5 days are used for resolution of diagnostic lines.	(mathematical techniques—subtraction of a local lf-trend—allow separating non-system variability caused by a regional factor).
Arctic Ocean (20)	A unique natural region with ice cover and a long polar night, which limits biological productivity. Ecosystems are qualitatively and quantitatively depleted and have a high sensitivity to external influences. Zooplankton composition is primarily represented by Arctic copepods: *Oithona similis* and *Oithona atlantica*, *Calanus finmarchicus* and *Calanus glacialis* (by biomass). The insolation mode is typical for high polar latitudes. In autumn-winter-spring periods the DHC is fixed on a suspension in a drift 10 m from the lower edge of the ice.	Spectral line structure; presence of diagnostic rhythms: c-rhythm (24 h) is preserved even in polar night conditions in the absence of solar insolation. Tidal synchronization is shown as the dv-rhythm (12 h), which supports the c-rhythm during periods without sunlight. The amplitude of the circadian rhythm decreases threefold with the onset of the polar night, but the rhythm still remains, which indicates the endogenous nature of the c-rhythm.	lf-rhythms are observed periodically. On a drift scale, it is determined by a change in course and temperature variations. In the local model, these factors together constitute one low-frequency harmonic with variable frequency.	Hypothesis 1 (spectral line structure and systematic component in the behavior of the autochthonous plankton community); hypothesis 2 (sufficiency of three spectral lines—lf-, c-, dv-lines—for the characteristic of plankton concentration oscillations); hypothesis 3 (mathematical techniques—subtraction of a non-system variability caused pollutants from regional factors, even with spectral intersection in mesoscale modality).

Three different hypotheses tested in this article are formulated at the end of the Section 1. Let us formulate them from the point of view of the spectral model of zooplankton biocenosis, when the Fourier spectrum of a number of zooplankton concentrations.

The functional interpolation of zooplankton concentrations in the form of a finite discrete Fourier series (Equation (2)) makes it possible to a priori accept the hypothesis of a line structure (not continuous) of the variability spectrum [54,56], the components of which are endogenously synchronized. The spectral line structure in the area of informative rhythms associated with vital activity and behavioral strategies is illustrated in Figure 4. This is related to the first hypothesis that we are checking.

The finiteness of the series, as well as the knowledge of environmental factors, allows, based on general considerations regarding rhythmic processes, building a heuristic biorhythmological model of zooplankton biocenosis. This model is based on piecewise continuous interpolation of experimental data segmented into three-five-seven day intervals related to mesoscale modality. By performing the formal Fourier analysis for the segments of the time series of zooplankton concentrations, we can obtain the amplitude, phase, period, constant component of variability serving the parameters of the interpolation dependence in Equations (1) and (2).

The second hypothesis discussed herein is that the set of intrinsic fluctuations necessary to adequately describe the variability of zooplankton biocenosis is bounded and known a priori for any water area and any biocenosis containing zooplankton. At the same time, we note that the dv-rhythm may be a harmonic of a nonsinusoidal diel cycle. Without excluding this alternative, we point out that in some cases—such as the Barents Sea and the polar night at SP-42—the dv-line persists or becomes stronger as the c-line weakens. This makes it difficult to explain the dv-rhythm solely as a harmonic but confirms its endogenous synchronization.

It is important for bioindication that these parameters of rhythmic processes of zooplankton organisms are sensitive to the impact of physical and chemical factors [26], electromagnetic and gravitational conditions.

The impact of pollutants causes epigenetic regulation—chemical changes that affect the function of their genes without changing their DNA.

In turn, epigenetic changes show a gradual response, becoming more pronounced as the causal factor increases or the time of its action is prolonged. Therefore, the concentration of pollutants causes chemical changes through these epigenetic mechanisms in the zooplankton individual. Daily cycles of individuals become less sensitive to environmental factors and ever more unregulated. Without the ability to respond to external signals, such as insolation, the zooplankters begin to rise to the surface at random times of the day, eventually destabilizing the entire food chain. This proposed explanation, drawn from the extensive chronobiology literature [38,40,60,74], describes an epigenetic pathway through which pollution may affect the living systems and points to an exogenous impact on the plankton biocenosis and its rhythm.

This means that pollution can be considered as one of the environmental parameters, along with lighting, temperature, salinity, etc., affecting the variability of the biotic community. An additional factor contributing to the drift of the SP-42 is the spatial variability of these parameters. A distinctive feature of pollution is the lack of rhythmicity of action; therefore, changes in biocenosis are non-rhythmic. Therefore, where it is not possible to separate the effects, we describe the transformation of local concentration data into the frequency domain (spectral representation) and the identification of periodic variability in local zooplankton concentration with an endogenous basis.

Diagnostics itself may be based on the mean concentration, amplitude, phase, and period of the selected rhythmic diagnostic processes. Anomalous changes in the spectrum, manifested as a nonsystematic disruption of rhythmicity, are regarded as exogenous factors. The task of identifying pollution then becomes one of diagnosing this nonsystematic variability [54,56]. The lf-component is used as an empirical correction for the physical trend associated with normal environmental factors that do not affect the quality of life of the biocenosis.

Thus, by using stress tests to demonstrate that mathematical methods and metrics can distinguish the pollutant-associated component of variability in plankton concentrations from exogenous variability driven by environmental factors—including a pronounced regional effect—we provide support for the third hypothesis (Table 4).

5. Conclusions

Based on the processing of 88 segments of three-day data on plankton concentrations, recorded in four different water areas, this study demonstrates that a bioindication station based on a submersible digital holographic camera (DHC) provides a means of in situ monitoring of zooplankton concentrations. These measurements provide local concentration, while the contributions of active movement and physical transport cannot be separated using unprocessed DHC data alone. Therefore, the data are subsequently interpreted using the spectral analysis and modeling with harmonic functions.

https://doi.org/10.3390/w18232985

The modeling of zooplankton community concentration utilizing harmonic temporal functions is predicated on the inherent self-organizing capacity of living systems. Consequently, such systems behave as autonomous oscillatory systems driven by an external synchronizing factor, which itself manifests as a harmonic oscillation. Unlike mechanical oscillators, biological systems are endowed with internal driving mechanisms—such as the organisms' nutritional needs—that sustain oscillations under external stimuli. These mechanisms are simple in nature (e.g., metabolic regulation) but are governed by complex biochemical processes colloquially referred to as biological clocks. Under this framework, we consider the rhythmic processes to possess an endogenous nature, maintaining steady fluctuations even when the external synchronizer diminishes or undergoes frequency drift (for example, daily variations in daylight length).

By illustrating the spectral structure of zooplankton concentration variability, based on data acquired via the DHC at five monitoring stations, we reveal a line spectral pattern characteristic of natural aquatic ecosystems. This simple mechanistic pattern, however, is complicated by the presence of multiple external synchronizers, which influence the biological system with varying phases, amplitudes, and frequencies. Such multifactorial external influences may obscure the bioindication studies. These include regional high-frequency s-rhythms, visualized as lf-lines over short temporal segments, reflecting the impact of high-frequency exogenous factors. Nonetheless, the cumulative effect of multiple factors remains bounded, resulting in a line spectral distribution in the frequency domain. Thus, the lf-component is used as an empirical correction for the physical trend.

By further developing the position regarding the limitation of the set of inherent fluctuations necessary for an adequate description of biocenosis variability, considering regional, hydro-physical, and biological differences, we demonstrate that three spectral lines (lf-, c-, dv-lines) are sufficient to characterize plankton concentration fluctuations. When describing zooplankton fluctuations through Equations (1, 2), the model becomes a priori known (it is in this sense that we call it the forecast model) due to the self-organizing nature of zooplankton biocenosis; the model parameters can then be derived from experimental data by applying the Fourier transform to the time series of zooplankton concentration.

This heuristic model is adaptive, as its scope is determined by the duration of the segment of the analyzed observation series. This, in turn, influences the modalities of environmental factors and the spectral transformation function used.

The third hypothesis, illustrated herein, posits the existence of mathematical techniques—such as the subtraction of the local trend of the lf-rhythm and the extension of the segment length—that enable the separation of non-systemic variability caused by pollutants from the regional factors, even in the presence of spectral intersection within the mesoscale modality (high-frequency s-rhythms).

This hypothesis is exemplified through two stress tests:

- controlled application of pollutants;
- discharge of organic waste during drift at the SP-42 station.

The observed changes in the model discrepancy concerning zooplankton biocenosis, induced by these stressors, serve as metrics that support the fact that the behavior of indigenous zooplankton can potentially function as a bioindicator of pollution. The primary diagnostic component (metric) in this context is the variability model, which relies on a priori knowledge of model parameters and the specific local conditions, particularly the influence of the lf-rhythm.

Building on the findings of this study, let us identify the following areas for future research, all of which fall beyond the scope of the present study:

- joint analysis of pressure in the medium and plankton concentration in longer series and in water areas with a different tidal rhythm;
- experimental confirmation of the turbulent nature of lf-rhythms in the mesoscale mode and analysis of the structure of the lf-component;
- assessment of the significance of diagnostic rhythms relative to an autocorrelated background in the bioindication process;
- study of the qualitative and quantitative dependence of the considered bioindicator markers on pollutant concentrations and environmental conditions.

Author Contributions: Conceptualization and methodology, V.D. and I.P.; software, A.D. and N.K.; investigation, A.D. and N.K.; formal analysis, N.K. and I.P.; validation, N.K. and A.D.; data curation, I.P.; resources and funding acquisition, V.D.; writing—original draft preparation, I.P.; writing—review and editing, V.D.; visualization, I.P., A.D., and N.K.; supervision and project administration, I.P. All authors have read and agreed to the published version of the manuscript.

Funding: This study was supported by the Development Program of Tomsk State University (Priority 2030).

Data Availability Statement: The raw data supporting the conclusions of this article will be made available by the authors on request.

Conflicts of Interest: The authors declare no conflicts of interest.

Abbreviations

The following abbreviations are used in this manuscript:

DHC	Digital Holographic Camera
CMOS	Complementary Metal-Oxide-Semiconductor
FOCL	Fiber Optical Communication Line
DNA	Deoxyribonucleic Acid
RMSD	Root Mean Square Deviation
SP-42	Severny Polyus-42

References

1. Boyd, P.W.; Arrigo, K.R.; Ardyna, M.; Halfter, S.; Huckstadt, L.; Kuhn, A.M.; Lannuzel, D.; Neukermans, G.; Novaglio, C.; Shadwick, E.H.; et al. The Role of Biota in the Southern Ocean Carbon Cycle. *Nat. Rev. Earth Environ.* **2024**, *5*, 390–408. https://doi.org/10.1038/s43017-024-00531-3.
2. Drago, L.; Panaïotis, T.; Irisson, J.O.; Babin, M.; Biard, T.; Carlotti, F.; Coppola, L.; Guidi, L.; Hauss, H.; Karp-Boss, L.; et al. Global Distribution of Zooplankton Biomass Estimated by In Situ Imaging and Machine Learning. *Front. Mar. Sci.* **2022**, *9*, 894372. https://doi.org/10.3389/fmars.2022.894372.
3. Steinberg, D.K.; Landry, M.R. Zooplankton and the Ocean Carbon Cycle. *Annu. Rev. Mar. Sci.* **2017**, *9*, 413–444. https://doi.org/10.1146/annurev-marine-010814-015924.
4. Vereshchaka, A. Navigating the Zooplankton Realm: Oceans of Diversity Beneath the Sea Surface. *Diversity* **2024**, *16*, 717. https://doi.org/10.3390/d16120717.
5. Chowdhury, P.; Khan, S.J.; Sumon, A.A.; El-regal, M.A.A.; Tayyamath, K.; Van Doan, H. The Role of Planktons in Sustaining the Function and Diversity of Marine Ecosystems: A Systematic Review. *Discov. Anim.* **2026**, *3*, 9.
6. Ostroumov, S.A. Biomachinery for Maintaining Water Quality and Natural Water Self-Purification in Marine and Estuarine Systems: Elements of a Qualitative Theory. *Int. J. Ocean. Oceanogr.* **2006**, *1*, 111–118.
7. Ostroumov, S.; Toderaş, I.; Ungureanu, L.; Miron, A.; Breahnă, A. Water Quality Formation and Improvement: The Key Role of Biological, Ecological and Biochemical Factors. *Buletinul Academiei de Ştiinţe a Moldovei* **2010**, *3*, 22–44.
8. Ostroumov, S.A. Polyfunctional role of biodiversity in processes leading to water purification: Current conceptualizations and concluding remarks. *Hydrobiologia* **2002**, *469*, 203–204. https://doi.org/10.1023/A:1015555022737.
9. Kozhov, M.M. *Biology of Lake Baikal*; Publishing house of Academy of Sciences of the USSR: Moscow, Russia, 1962; 315p.

10. Kozhova, O.M.; Mel'nik, N.G. On the issue of the cyclical nature of the process of long-term fluctuations in zooplankton biomass in Lake Baikal. *Hydrobiol. J.* **1977**, *13*, 36–39.
11. Shadrin, N.V.; Anufriieva, E.V. An ecosystem role of spatial and temporal inhomogeneity in feeding of plankton crustaceans. *Ekosystemy* **2018**, *14*, 119–128.
12. Rzhepka, T.; Rzhepka, E. Some Aspects of Studying Zooplankton as a Bioindicator of the Ecological State of Lake Baikal. *Bull. Baikal State Univ.* **2024**, *34*, 538–546. https://doi.org/10.17150/2500-2759.2024.34(3).538-546.
13. Leibold, M.; Norberg, J. Biodiversity in Metacommunities: Plankton as Complex Adaptive Systems? *Limnol. Oceanogr.* **2004**, *49*, 1278–1289. https://doi.org/10.4319/lo.2004.49.4_part_2.1278.
14. D'Alelio, D. Biological Complexity behind Plankton System Functioning: Synthesis and Perspectives from a Marine Long Term Ecological Research. *Adv. Oceanogr. Limnol.* **2017**, *8*, 187–198. https://doi.org/10.4081/aiol.2017.7194.
15. Uddin, M.G.; Nash, S.; Rahman, A.; Olbert, A.I. A comprehensive method for improvement of water quality index (WQI) models for coastal water quality assessment. *Water Res.* **2022**, *219*, 118532. https://doi.org/10.1016/j.watres.2022.118532.
16. Swain, L.G. The evolution of the Canadian (CCME) Water Quality Index. *Water Qual. Res. J.* **2024**, *59*, 342–346. https://doi.org/10.2166/wqrj.2024.052.
17. Lestari, T.A.; Adriman, A.; Fauzi, M. Water Quality Status In Tanjung Buton Port Area Based On Sea Water Quality Index (IKAL). *J. Enviromental Eng. Sustain. Technol.* **2024**, *11*, 103–110. https://doi.org/10.21776/ub.jeest.2024.011.02.4.
18. Nguyen, T.G.; Thi, N.; Huynh, H. Evaluating Surface Water Quality Using Indexes of Water Quality and Plankton Diversity. *Civ. Eng. J.* **2023**, *9*, 1187–1202. https://doi.org/10.28991/CEJ-2023-09-05-011.
19. Muhamedieva, D.T.; Niyozmatova, N.A. Assessment of the ecological state of a water body for biodiversity monitoring according to biological and hydrochemical indicators. *E3S Web Conf.* **2023**, *411*, 02043. https://doi.org/10.1051/e3sconf/202341102043.
20. Lachowicz, J.; Szopa, A.; Ignatiuk, K.; Świąder, K.; Serefko, A. Zebrafish as an Animal Model in Cannabinoid Research. *Int. J. Mol. Sci.* **2023**, *24*, 10455. https://doi.org/10.3390/ijms241310455.
21. Rajewicz, W.; Helmer, N.; Schmickl, T.; Thenius, R. Living Organisms as Sensors for Biohybrid Monitoring Systems. In *Lecture Notes in Computer Science (Including Subseries Lecture Notes in Artificial Intelligence and Lecture Notes in Bioinformatics)*; Springer Nature: Cham, Switzerland, 2023; Volume 14158, pp. 348–362. https://doi.org/10.1007/978-3-031-39504-8_24.
22. Chandel, P.; Mahajan, D.; Thakur, K.; Kumar, R.; Kumar, S.; Brar, B.; Sharma, D.; Sharma, A.K. A Review on Plankton as a Bioindicator: A Promising Tool for Monitoring Water Quality. *World Water Policy* **2024**, *10*, 213–232. https://doi.org/10.1002/wwp2.12137.
23. Directive 2000/60/EC of the European Parliament and of the Council of 23 October 2000 Establishing a Framework for Community Action in the Field of Water Policy. Available online: https://eur-lex.europa.eu/eli/dir/2000/60/oj (accessed on 25 September 2026).
24. Pinna, M.; Zangaro, F.; Saccomanno, B.; Scalone, C.; Bozzeda, F.; Fanini, L.; Specchia, V. An Overview of Ecological Indicators of Fish to Evaluate the Anthropogenic Pressures in Aquatic Ecosystems: From Traditional to Innovative DNA-Based Approaches. *Water* **2023**, *15*, 949. https://doi.org/10.3390/w15050949.
25. Boldrocchi, G.; Villa, B.; Monticelli, D.; Spanu, D.; Magni, G.; Pachner, J.; Mastore, M.; Bettinetti, R. Zooplankton as an Indicator of the Status of Contamination of the Mediterranean Sea and Temporal Trends. *Mar. Pollut. Bull.* **2023**, *197*, 115732. https://doi.org/10.1016/j.marpolbul.2023.115732.
26. Aschoff, J. A Survey on Biological Rhythms. In *Biological Rhythms*; Springer: Boston, MA, USA, 1981; pp. 3–10. https://doi.org/10.1007/978-1-4615-6552-9_1.
27. Zhang, L.; Hastings, M.H.; Green, E.W.; Tauber, E.; Sladek, M.; Webster, S.G.; Kyriacou, C.P.; Wilcockson, D.C. Dissociation of Circadian and Circatidal Timekeeping in the Marine Crustacean Eurydice Pulchra. *Curr. Biol.* **2013**, *23*, 1863–1873. https://doi.org/10.1016/j.cub.2013.08.038.
28. Zantke, J.; Ishikawa-Fujiwara, T.; Arboleda, E.; Lohs, C.; Schipany, K.; Hallay, N.; Straw, A.D.; Todo, T.; Tessmar-Raible, K. Circadian and Circalunar Clock Interactions in a Marine Annelid. *Cell Rep.* **2013**, *5*, 99–113. https://doi.org/10.1016/j.celrep.2013.08.031.
29. Mirick, D.K.; Davis, S. Melatonin as a biomarker of circadian dysregulation. *Cancer Epidemiol. Biomark. Prev.* **2008**, *17*, 3306–3313. https://doi.org/10.1158/1055-9965.EPI-08-0605.
30. Njus, D.; Sulzman, F.M.; Hastings, J.W. Membrane model for the circadian clock. *Nature* **1974**, *248*, 116–120. https://doi.org/10.1038/248116a0.
31. Sweeney, B.M. A physiological model for circadian rhythms derived from the acetabularia rhythm paradoxes. *Int. J. Chronobiol.* **1974**, *2*, 25–33.

32. Sweeney, B.M.; Borgese, M.B. A Circadian Rhythm In Cell Division In A Prokaryote, The Cyanobacterium Synechococcus WH7803 1. *J. Phycol.* **1989**, *25*, 183–186. https://doi.org/10.1111/j.0022-3646.1989.00183.x.
33. Holzberg, D.; Albrecht, U. The Circadian Clock: A Manager of Biochemical Processes Within the Organism. *J. Neuroendocrinol.* **2003**, *15*, 339–343. https://doi.org/10.1046/j.1365-2826.2003.00992.x.
34. Halberg, F.; Katinas, G.S. Chronobiologic glossary of the International Society for the Study of Biologic Rhythms. *Int. J. Chronobiol.* **1973**, *1*, 31–63.
35. Steele, J.H.; Henderson, E.W. The role of predation in plankton models. *J. Plankton Res.* **1992**, *14*, 157–172. https://doi.org/10.1093/plankt/14.1.157.
36. Scheffer, M. Should we expect strange attractors behind plankton dynamics—And if so, should we bother? *J. Plankton Res.* **1991**, *13*, 1291–1305. https://doi.org/10.1093/plankt/13.6.1291.
37. Medvinskii, A.B.; Petrovskii, S.V.; Tikhonova, I.A.; Tikhonov, D.A.; Li, B.-L.; Venturino, E.; Malchow, H.; Ivanitskii, G.R. Spatio-Temporal Pattern Formation, Fractals, and Chaos in Conceptual Ecological Models as Applied to Coupled Plankton-Fish Dynamics. *Physics-Uspekhi* **2002**, *45*, 27–57. https://doi.org/10.1070/PU2002v045n01ABEH000980.
38. Pittendrigh, C.S. Circadian Rhythms and the Circadian Organization of Living Systems. *Cold Spring Harb. Symp. Quant. Biol.* **1960**, *25*, 159–184. https://doi.org/10.1101/SQB.1960.025.01.015.
39. Soviadan, Y.D.; Benedetti, F.; Brandão, M.C.; Ayata, S.-D.; Irisson, J.-O.; Jamet, J.L.; Kiko, R.; Lombard, F.; Gnandi, K.; Stemmann, L. Patterns of Mesozooplankton Community Composition and Vertical Fluxes in the Global Ocean. *Prog. Oceanogr.* **2022**, *200*, 102717. https://doi.org/10.1016/j.pocean.2021.102717.
40. How Road Salt and Other Environmental Pollution Disrupts the Circadian Rhythm. Available online: https://www.chronobiology.com/how-road-salt-and-other-environmental-pollution-disrupts-the-circadian-rhythm/ (accessed on 1 June 2022).
41. Dyomin, V.; Polovtsev, I.; Kurkova, D.; Davydova, A. Modalities and Trends of Variability of Plankton Concentrations Recorded During a Digital Holographic Experiment In Situ. *Water* **2025**, *17*, 3365. https://doi.org/10.3390/w17233365.
42. Apel, J.R.; Byrne, H.M.; Proni, J.R.; Charnell, R.L. Observations of oceanic internal and surface waves from the earth resources technology satellite. *J. Geophys. Res.* **1975**, *80*, 865–881. https://doi.org/10.1029/JC080i006p00865.
43. Apel, J.R. Linear and nonlinear internal waves in coastal and marginal seas. *In Oceanographic Application of Remote Sensing*; CRC Press, Inc.: Boca Raton, FL, USA, 1995; pp. 57–78.
44. Apel, J.R. Oceanic internal waves and solitons. In *Synthetic Aperture Radar User's Manual*; NOAA: Washington, DC, USA, 2004; Chapter 7, pp. 189–206.
45. Menshutkin, V.V.; Rukhovets, L.A.; Filatov, N.N. Ecosystem modeling of freshwater lakes (Review): 1. Hydrodynamics of lakes. *Water Resour.* **2013**, *40*, 606–620. https://doi.org/10.1134/S0097807813060080.
46. Flierl, G.; McGillicuddy, D.J. Mesoscale and Submesoscale Physical—Biological Interactions. In *The Sea*; Robinson, A.R., McCarthy, J.J., Rothschild, B.J., Eds.; John Wiley & Sons, Inc.: New York, NY, USA, 2002; Volume 12, pp. 113–186.
47. Pollina, T.; Larson, A.G.; Lombard, F.; Li, H.; Le Guen, D.; Colin, S.; de Vargas, C.; Prakash, M. PlanktoScope: Affordable Modular Quantitative Imaging Platform for Citizen Oceanography. *Front. Mar. Sci.* **2022**, *9*, 949428. https://doi.org/10.3389/fmars.2022.949428.
48. Orenstein, E.C.; Ratelle, D.; Briseño-Avena, C.; Carter, M.L.; Franks, P.J.S.; Jaffe, J.S.; Roberts, P.L.D. The Scripps Plankton Camera System: A Framework and Platform for in Situ Microscopy. *Limnol. Oceanogr. Methods* **2020**, *18*, 681–695. https://doi.org/10.1002/lom3.10394.
49. Merz, E.; Kozakiewicz, T.; Reyes, M.; Ebi, C.; Isles, P.; Baity-Jesi, M.; Roberts, P.; Jaffe, J.S.; Dennis, S.R.; Hardeman, T.; et al. Underwater Dual-Magnification Imaging for Automated Lake Plankton Monitoring. *Water Res.* **2021**, *203*, 117524. https://doi.org/10.1016/j.watres.2021.117524.
50. Calbet, A. Sampling Plankton. In *The Wonders of Marine Plankton*; Springer Nature: Cham, Switzerland, 2024; pp. 131–136. https://doi.org/10.1007/978-3-031-50766-3_22.
51. Skjoldal, H.R. Species composition of three size fractions of zooplankton used in routine monitoring of the Barents Sea ecosystem. *J. Plankton Res.* **2021**, *43*, 762–772. https://doi.org/10.1093/plankt/fbab056.
52. Panaiotis, T. Plankton Distribution Across Scales: Contributions from Artificial Intelligence to Plankton Ecology. 2023. Available online: https://theses.hal.science/THESES-SU/tel-04151175v1 (accessed on 25 September 2026).
53. Williamson, F.; van den Broeke, J.; Koster, T.; Klein Koerkamp, M.; Verhoef, J.W.; Hoogterp, J.; Trietsch, E.; de Graaf, B.R. Online water quality monitoring in the distribution network. *Water Pract. Technol.* **2014**, *9*, 575–585. https://doi.org/10.2166/wpt.2014.064.

54. Dyomin, V.; Davydova, A.; Kirillov, N.; Kondratova, O.; Morgalev, Y.; Morgalev, S.; Morgaleva, T.; Polovtsev, I. Monitoring Bioindication of Plankton through the Analysis of the Fourier Spectra of the Underwater Digital Holographic Sensor Data. *Sensors* **2024**, *24*, 2370. https://doi.org/10.3390/s24072370.
55. Dyomin, V.; Morgalev, Y.; Polovtsev, I.; Morgalev, S.; Morgaleva, T.; Davydova, A.; Kondratova, O. Phototropic Behavioral Responses of Zooplankton in Lake Baikal In Situ and during the Anthropogenic Impact Modeling. *Water* **2023**, *15*, 2957. https://doi.org/10.3390/w15162957.
56. Dyomin, V.; Polovtsev, I.; Davydova, A.; Kirillov, N. Spectroscopic aspects of underwater digital holography of plankton. *Sci. Rep.* **2025**, *15*, 1884. https://doi.org/10.1038/s41598-025-85790-w.
57. Dyomin, V.; Kurkova, D.; Davydova, A.; Polovtsev, I.; Morgalev, S. Plankton Concentration Model Consistent with Natural Events and Monitoring Series of Holographic Measurements. *J. Mar. Sci. Eng.* **2025**, *13*, 140. https://doi.org/10.3390/jmse13010140.
58. Dyomin, V.V.; Davydova, A.Y.; Morgalev, S.Y.; Kirillov, N.S.; Olshukov, A.; Polovtsev, I.; Davydov, S. Monitoring of Plankton Spatial and Temporal Characteristics With the Use of a Submersible Digital Holographic Camera. *Front. Mar. Sci.* **2020**, *7*, 653. https://doi.org/10.3389/fmars.2020.00653.
59. Otnes, R.K.; Enochson, L.D. *Applied Time Series Analysis, Vol. 1: Basic Techniques*; John Wiley & Sons Inc.: New York, NY, USA, 1978.
60. Challet, E. The circadian regulation of food intake. *Nat. Rev. Endocrinol.* **2019**, *15*, 393–405. https://doi.org/10.1038/s41574-019-0210-x.
61. Neumann, J.; Kaiser, T.S. Lunar and Tidal Rhythms and Clocks. In *Insect Chronobiology. Entomology Monographs*; Springer: Singapore, 2023; pp. 203–227. https://doi.org/10.1007/978-981-99-0726-7_10.
62. Rusetskaya, G.; Sanina, L. The Role and Importance of Protected Forest Areas in the Preservation of Lake Baikal. *Bull. Baikal State Univ.* **2024**, *34*, 96–108. https://doi.org/10.17150/2500-2759.2024.34(1).96-108.
63. Tereza, E.P.; Naumova, E.Y.u.; Belykh, O.I.; Logacheva, N.F.; Pomazkova, G.I.; Dzyuba, Y.e.V.; Melnik, N.G. Vertical Distribution and Feeding Activity of Epischura Baicalensis Sars (Copepoda) Nauplii in Response to Two Predators in Lake Baikal in Winter. *Fundam. Appl. Limnol.* **2007**, *169*, 211–216. https://doi.org/10.1127/1863-9135/2007/0169-0211.
64. *ISO 6341:2012*; Preview Water Quality—Determination of the Inhibition of the Mobility of *Daphnia magna* Straus (Cladocera, Crustacea)—Acute Toxicity Test. ISO: Geneva, Switzerland, 2012.
65. Tulokhonov, A.K.; Garmaev, Y.Z.; Tsydypov, B.Z. Spatial and Temporal Dynamics of the Baikal Coastal Line Caused by Control of the Lake Level Regime. *Geogr. Environ. Sustain.* **2013**, *6*, 20–27. https://doi.org/10.24057/2071-9388-2013-6-2-20-27.
66. Shimarayev, M.N.; Starygina, L.N. Lake Baikal: Zonal atmospheric circulation, climate and hydrological processes (1968–2007). *Geogr. Nat. Resour.* **2010**, *31*, 245–250. https://doi.org/10.1016/j.gnr.2010.09.009.
67. Bondarenko, N.A.; Sheveleva, N.G.; Poberezhnaya, A.E.; Pen'kova, O.G. Main parameters of the spring plankton spatial distribution, Lake Baikal, by the 2023 observations. *Proc. Mordovia State Nat. Reserve* **2025**, *36*, 39–56. https://doi.org/10.24412/cl-31646-2686-7117-2025-36-39-56.
68. Voronkov, P.P.; Uralov, N.S.; Chernovskaya, E.N. The main features of the hydrochemical regime of the coastal zone of Central Murman. *Trudy Murmanskoy Biologicheskoy Stantsii* **1978**, *1*, 39–102.
69. Il'in, G.V.; Nalbandov, Y.R.; Savinova, T.N. Hydrological characteristics of water masses in the coastal zone of Eastern Murman. In *Zakonomernosti Bioproduktsionnyh Protsessov v Barentsevom More*; Bryazgina, V.F., Bobrova, Y.A., Fomina, O.K., Eds.; Izd-vo KF AN SSSR: Apatity, Russia, 1978; pp. 3–13.
70. Il'in, G.V.; Moiseev, D.V.; Shirokolobov, D.V.; Deryabin, A.A.; Pavlova, L.G. Long-term dynamics of hydrological conditions of the Zelenetskaya Bay, East Murman. *Vestn. MGTU* **2016**, *19*, 268–277.
71. Arashkevich, E.G. Zooplankton the Barents Sea. In *The Barents Sea System*; Shirshov Institute of Oceanology Publishing House: Moscow, Russia, 2021; pp. 331–351. https://doi.org/10.29006/978-5-6045110-0-8/(26).
72. NOAA. What Are Spring and Neap Tides? Available online: https://oceanservice.noaa.gov/facts/springtide.html (accessed on 17 November 2024).

73. Kosobokova, K.; Hirche, H.-J. Zooplankton distribution across the Lomonosov Ridge, Arctic Ocean: Species inventory, biomass and vertical structure. *Deep Sea Res. Part I Oceanogr. Res. Pap.* **2000**, *47*, 2029–2060. https://doi.org/10.1016/S0967-0637(00)00015-7.
74. Hurley, J.M. Can Road Salt and Other Pollutants Disrupt Our Circadian Rhythms? 2018. Available online: https://theconversation.com/can-road-salt-and-other-pollutants-disrupt-our-circadian-rhythms-89211 (accessed on 25 September 2026).

Disclaimer/Publisher's Note: The statements, opinions and data contained in all publications are solely those of the individual author(s) and contributor(s) and not of MDPI and/or the editor(s). MDPI and/or the editor(s) disclaim responsibility for any injury to people or property resulting from any ideas, methods, instructions or products referred to in the content.